

# What is glacier sliding?

Robert LAW<sup>1,2</sup>, David CHANDLER<sup>3,2</sup>, Andreas BORN<sup>1,2</sup>

<sup>1</sup>*Department of Earth Science, University of Bergen, Bergen, Norway*

<sup>2</sup>*Bjerknes Centre for Climate Research, Bergen, Norway*

<sup>3</sup>*NORCE Norwegian Research Centre, Bergen, Norway*

<robert.law@uib.no>

## ABSTRACT.

Glacier and ice-sheet motion is fundamental to glaciology. However, there is still no clear consensus for the optimal way to describe the sliding component of glacier and ice-sheet dynamics. Typically, sliding is parameterised using a traction coefficient nominally linked to a given theory describing one or a limited set of sliding processes. However, this approach precludes the possibility of multiple simultaneous and spatio-temporally varying sliding modes with inaccuracies resulting in model error propagation as the system evolves away from the conditions under which it was optimised for. Here, revisiting early theoretical work, we describe glacier sliding as a scale- and setting-dependent ‘inner flow’ that arises from multiple overlapping sub-processes, including viscous ice deformation and obstacle resistance (or ‘form drag’), thereby bridging divides between hard and soft beds and rough and smooth beds. The corresponding ‘outer flow’ then accounts for ice deformation that is only minimally influenced by bed properties. We propose that the importance of ‘Iken’s bound’ can then be significantly reduced if viscous ice deformation becomes a significant process in a given region within the inner flow, which may explain the persistent functionality of power-law sliding in large-scale process-agnostic sliding studies over rough topography. Last, reviewing observation-based studies and considering the sheer diversity of sliding processes, we suggest that a simple ‘unified’ sliding relationship controlled by a single tunable coefficient may not be realistic. However, we show that given reasonable assumptions, all sliding relationships should fall somewhere between regularised-Coulomb and power-law end members, and that a power-law, or compound relationship with careful consideration of the power value may provide the most flexible way to account for the varied net effect of compound sliding sub-processes.

## 1 BACKGROUND

*The question then occurs, is the viscosity real or apparent?*  
**John Tyndall on glacier motion in 1857.**

Glacier sliding is a phenomenologically distinct problem within earth sciences, separated from simpler plane-on-plane sliding problems between two elastic solids by multiple confounding factors. The relative softness of ice allows for both viscous deformation under a non-Newtonian power-law *and* discrete slip at the ice-bed interface, which may occur in a stick-slip or continuous manner. A ‘soft’ sediment phase provides a further medium to convey deformation in many instances (and is shaped in turn by glacial processes), while ‘hard’ underlying bedrock can constitute a highly topographically irregular base ranging from <1 cm asperities to dra-

matic fjords, necessitating ice deformation around rigid obstacles over length scales covering 5 orders of magnitude. A subglacial hydrological system comprised largely of melted ice may significantly alter the effective pressure of the ice upon its substrate, and influence the roughness and material characteristics of the base itself. Debris entrained within basal ice interacts with the subglacial environment and influences both basal ice properties and the frictional properties of the glacier sole. These considerations present a wide parameter space for basal boundary conditions, which may also exhibit considerable spatial and temporal variations. The net outcome is significant difficulty in the derivation of a ‘unified’ or ‘generalised’ sliding relationship, usually expressed in the form

$$\tau_b = f(u_b) \text{ or } \tau_b = f(u_b, N) \quad (1)$$

where  $\tau_b$  is basal traction,  $u_b$  is ice velocity tangential to the ice-bed interface,  $N = P_i - P_w$  is effective pressure,  $P_w$  is subglacial water pressure, and  $P_i$  is the ice overburden pressure (or with  $u_b$  and  $\tau_b$  vectorised for higher dimensions, e.g. 9).

Determining an appropriate sliding relationship is central to producing tractable, physically-based projections of the contribution of ice sheets and glaciers to sea-level rise and fresh-water fluxes over the coming centuries. Extant sliding relationships (Fig. 1, Table. 1) influence ice-sheet model output at catchment to entire ice sheet scales, with the distinction between bounded traction (plastic, regularised-Coulomb) and unbounded traction (all other relationships) being particularly consequential (Gillet-Chaulet and others, 2012; Parizek and others, 2013; Ritz and others, 2015; Tsai and others, 2015; Bons and others, 2018; Kyrke-Smith and others, 2018; Lippert and others, 2024; Trevers and others, 2024), resulting in up to a 100% increase in mass loss over 100 years dependent on initialisation (Brondex and others, 2019; Åkesson and others, 2021). Nonetheless, around five<sup>1</sup> (Section 3) sliding relationships implicitly or explicitly capturing different sliding processes are used in the Ice Sheet Model Intercomparison Project (ISMIP) models (Goelzer and others, 2020; Seroussi and others, 2020), which guide worldwide policy on sea level rise mitigation. This state of affairs is not immediately straightforward to resolve, as the inverse methods that tune for  $C$ , the ‘traction coefficient’, will produce reasonable basal stress states whichever equation in Table 1 is chosen as the global stress balance condition must be met (Joughin and others, 2009; Arthern and Gudmundsson, 2010). There is therefore no simple approach to discounting sliding relationships given solely a snapshot of glacier or ice sheet velocity and geometry. Errors associated with an inappropriate choice of basal sliding relationship subsequently increase as a function of model run time (Aschwanden and others, 2021).

In numerical ice-sheet models, these sliding relationships form a critical thread between the processes occurring at the sub-grid-scale and the numerical solution defined at the grid scale (where ‘grid’ refers to discretised model grid cells or mesh elements)<sup>2</sup>. In discretised continuum mechanics models, the distinction between sub-grid-scale and grid-scale is

<sup>1</sup>Some sliding relationships can be considered a simplified versions of one another. For example power-law and pseudo-plastic can be manipulated into linear or plastic relationships, the  $N$  in Budd sliding is effectively subsumed into the  $C$  of power-law sliding during inversion if it is assumed that subglacial water pressure does not vary in time, making this number subjective.

<sup>2</sup>This was not always the case, with purely analytical sliding relationships predating the first numerical models by decades (Weertman, 1957; Rasmussen and Campbell, 1973; Jenssen, 1977) which may explain why sub-grid-scale processes were not initially a concern.

| Sliding relationship         | Equation   |
|------------------------------|--|
| Linear <sup>†</sup>          | $\tau_b = C u_b$ or $\tau_b = N C u_b$                     |
| Plastic <sup>†</sup>         | $\tau_b = C$ or $\tau_b = C N$                             |
| Weertman(-type) <sup>†</sup> | $\tau_b = C u_b^{\frac{2}{1+n}}$ or $\tau_b = C u_b^{1/m}$ |
| Pseudo-plastic <sup>†</sup>  | $\tau_b = \tau_c \frac{u_b^{1/m}}{u_t^{1/m}}$              |
| Budd <sup>†</sup>            | $\tau_b = C (N^q u_b)^{1/m}$ or $\tau_b = C N u_b^{1/m}$   |
| Regularised-Coulomb          | $\tau_b = C \left( \frac{u_b}{u_b + u_t} \right)^{1/m}$    |

**Table 1. Selected sliding relationships applied in numerical glacier and ice-sheet models, expressed in one-dimensional form.** <sup>†</sup> Denotes that the sliding relationship is used in Goelzer and others (2020) or Seroussi and others (2020) ISMIP experiments. In all equations  $\tau_b$  is basal traction and  $u_b$  is the basal velocity tangential to the bed. Where present,  $n$  is the exponent used in Glen’s flow law (usually 3) and is only used where an explicit link to Glen’s flow law is made in the paper proposing the sliding relationship,  $m$  is an exponent often related to Glen’s flow law, but not always explicitly,  $N$  is the effective pressure,  $C$  is the traction coefficient which may be adapted from its use in the original paper for simplified intercomparison (for example we replace  $1/C$  with  $C$  in the Budd relationship),  $\tau_c$  is the yield stress in the pseudo-plastic relationship,  $q$  is a fitting parameter in the Budd relationship, and  $u_t$  is the threshold velocity in the pseudo-plastic and regularised-Coulomb relationships. The rate-weakening 2D cavities relationship in Fig. 1 is not included, as no numerical ice-sheet or glacier models include rate-weakening behaviour above a given velocity threshold. Depending on convention, the RHS may be negative in the original paper to indicate a traction force opposite to velocity direction. In dimensions higher than 1 the sliding relationship is vectorised (e.g. Eq. ??). **Notes: Linear:** Adapted from Nye (1969) and Kamb (1970). As applied in e.g. Morlighem and others (2013). The version with  $N$  is used in some Goelzer and others (2020) experiments. **Weertman:** Equation featuring  $n$  is adapted from Weertman (1957) where  $n$  is set as 3.  $m$  is often used in models instead of  $n$  where  $m$  is usually between 3 and 4. **Pseudo-plastic:** Effectively the same as Weertman but included for frequent use in PISM applications e.g. Aschwanden and others (2016), the pseudo-plastic relationship can be varied between plastic ( $m = \infty$ ), linear ( $m = 1$ ), or power-law ( $2 \leq m \leq 4$ ) behaviour. **Regularised-Coulomb:** The simplest form excluding  $N$ , adapted from (Joughin and others, 2019). Other formulations exist such as  $\tau_b = C u_b N \left( \frac{u_b^{-n+1}}{u_b + A_s C^n N^n} \right)^{1/n}$  (Helanow and others, 2021) where  $A_s$  is a parameter specific to this formulation. The differences between regularised-Coulomb relationships are not negligible (Fig. A1). **Plastic:** As used in e.g. Bougamont and others (2014) and the PISM default (Winkelmann and others, 2011). **Budd:** As developed in Budd and others (1984) where  $q = 1$  and  $m = 3$  and used in Budd and Jacka (1989) with  $q = 2$  and  $m = 1$ . The alternative and simplified Budd formulation is as used in Choi and others (2022). The proposal of Tsai and others (2021) also bears similarities with Budd sliding.

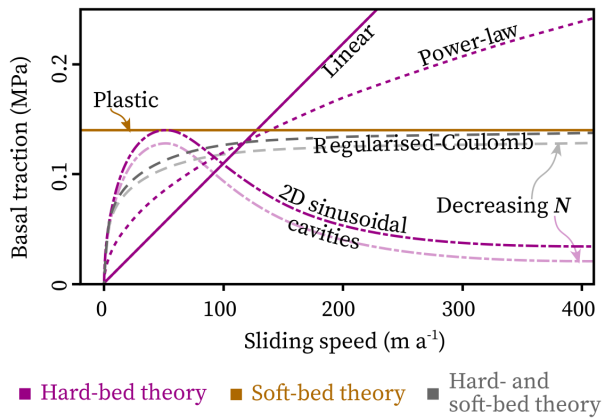


**Fig. 1. Existing sliding parameterisations and how their development relates to soft- and hard-bed theory.** Traction and velocity values are plausible, but for illustrative purposes only.

usually made using a ‘representative volume element’ that is large enough to be representative of the bulk behaviour of micro-scale processes within the constitutive material it represents. For ice deformation, this is straightforward – an ice volume of  $1 \text{ m}^3$ , much below the resolution of even the most detailed numerical models, will contain sufficient variability in crystal orientation, size, and impurities as to have effectively the same response to an applied stress field as a different  $1 \text{ m}^3$  of the same material. Lab-based experiments using small volumes of ice (e.g. Glen, 1952) can therefore be reasonably applied to much larger-scale models, even if separate issues such as the importance of tertiary creep remain (Adams and others, 2021).

There is not, however, an obvious representative volume, or ‘representative surface’ element size for glacier sliding processes, with investigations into glacier sliding covering a disparate range of scales extending over seven orders of magnitude from millimetres to 10s of kilometres (Fig. 2). For example, lab experiments for ice-sediment shearing behaviour may be conducted at a scale of tens of centimetres (e.g. Iverson and others, 1998; Zoet and Iverson, 2020), up-scaled to field settings covering an entire glacier where subglacially entrained clasts, variable subglacial hydrology, or bedrock obstacles further influence the relationship between traction and velocity (e.g. Iverson and others, 1995; Hedfors and others, 2003; Gimbert and others, 2021), and ultimately applied to ice-sheet models where individual grid cells can exceed 10s of kilometres (or have a highly variable size across a given domain) and cover an uncertain and/or heterogeneous subglacial landscape (e.g. Kyrke-Smith and others, 2018; Holschuh and others, 2020; Paxman and others, 2021). Nonetheless, routinely-used sliding parameteri-

sations in ice sheet models almost exclusively use theories derived for one or a limited set of sliding processes at small scales (Goelzer and others, 2020; Seroussi and others, 2020), without representing the full range of scale-dependent processes.

Representation of sliding in glacier and ice-sheet models is further hindered by a tendency to classify the bed either as ‘soft’ (less rigid than ice and subject to sediment deformation and transport under glacier slip and subglacial hydrology even at short time scales) or ‘hard’ (more rigid than ice and only appreciably modified by sliding or hydrology at glacial-cycle time scales). Glacier and ice-sheet models generally cannot represent settings that may feature both soft- and hard-bed characteristics within a single grid cell or across a model domain (Fig. 3). This ‘one or the other’ classification is challenged by geological and geomorphological evidence of mixed soft- and hard-bed regions in both recently deglaciated landscapes (e.g. Hogan and others, 2020; Garcia-Oteyza and others, 2022) and in active subglacial settings (Jordan and others, 2023) but has received very little attention in glaciological studies (Koellner and others, 2019). A middle-ground between hard and soft beds can also exist if the substrate is only deformable under certain conditions, i.e. very thick ice cover with high subglacial water pressure. Sub-grid-scale topography is furthermore known to significantly influence ice flow (Kyrke-Smith and others, 2018; Hoffman and others, 2022; Law and others, 2023), and may even dominate grid-scale basal traction (Fig. 3b), but is also lacking from present sliding parameterisations.

In this paper we provide a clear framework for describing glacier sliding as behaviour emerging from multiple scale- and setting-dependent processes (summarised in Fig. 4), rather than as a single dominant process. We reconsider the ‘inner-outer’ flow division (Section 2) first proposed by Fowler (1977), but with a more universal approach to the inclusion of numerous sliding sub-processes over three dimensions and resistance from sub-grid-scale topography (Section 3). We briefly cover standard soft- and hard-bed theory (Sections 3.1 and 3.2); form drag, roughness, and temperate ice (Section 3.3); stick-slip vs. continuous sliding (Section 3.5); the overlap between soft- and hard-bed sliding (Section 3.6); the basal ice layer and ice rheology (Section 3.4); and how these sub-processes are modified by subglacial hydrology (Section 4). We focus on annual timescales as these are the most relevant for predictive and palaeo models, and largely avoid the transient influence of e.g. supraglacial lake drainages (Das and others, 2008), rainfall events (Doyle and others, 2015), or seasonal modulation (Bartholomew and others, 2011; Sole and others, 2013). In Section 5 we review process-agnostic studies fitting sliding relationships to observational data. Last,

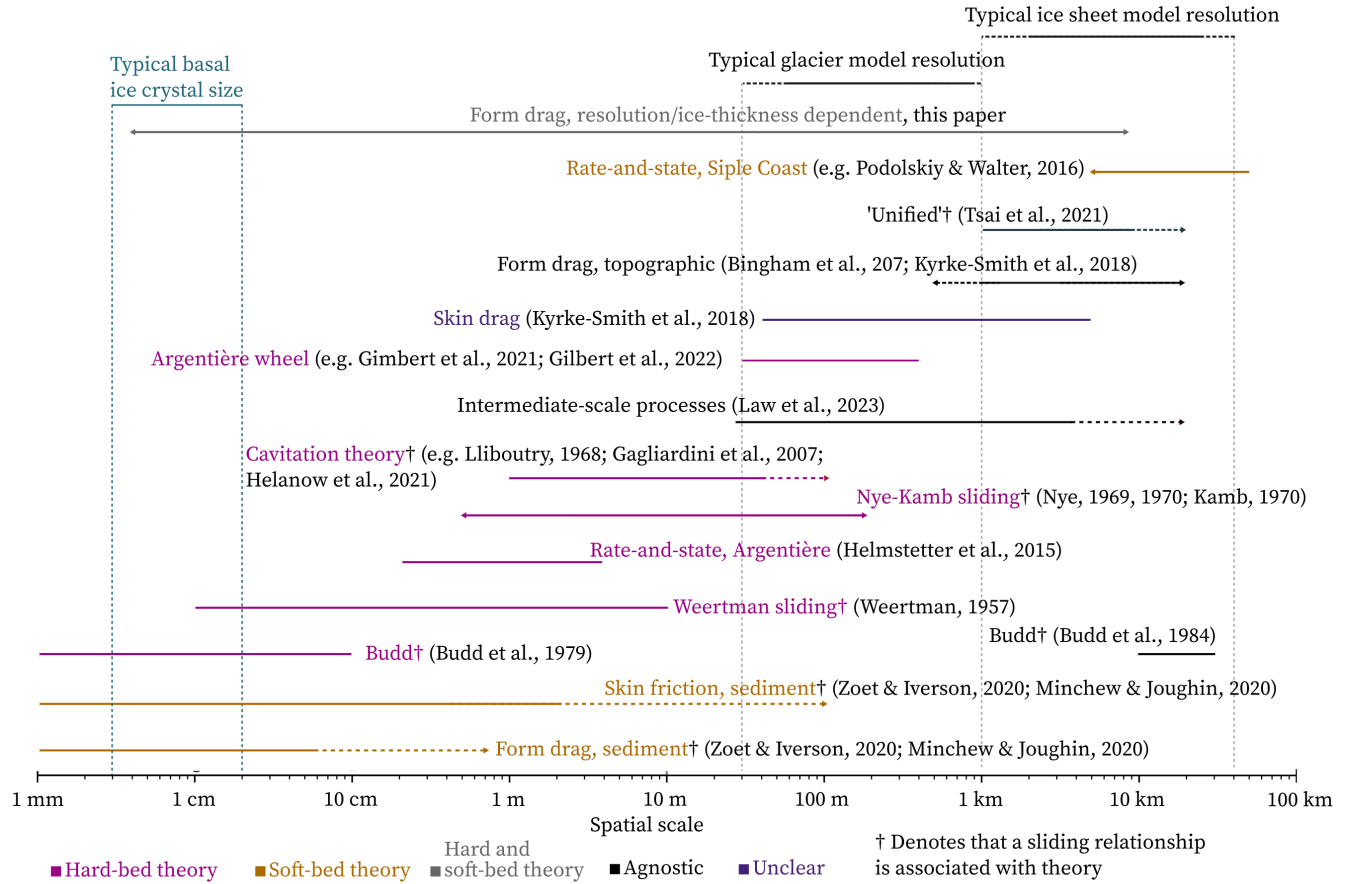


**Fig. 2. Spatial scales for theories and parameterisations of basal sliding.** A solid line indicates coverage as explicitly defined in the associated paper while a dashed line indicates probable situation dependent coverage and an arrow indicates extension beyond the scale bar or an uncertain coverage beyond the given limit. Reasoning behind the positioning of each spatial range is provided in Appendix A2.

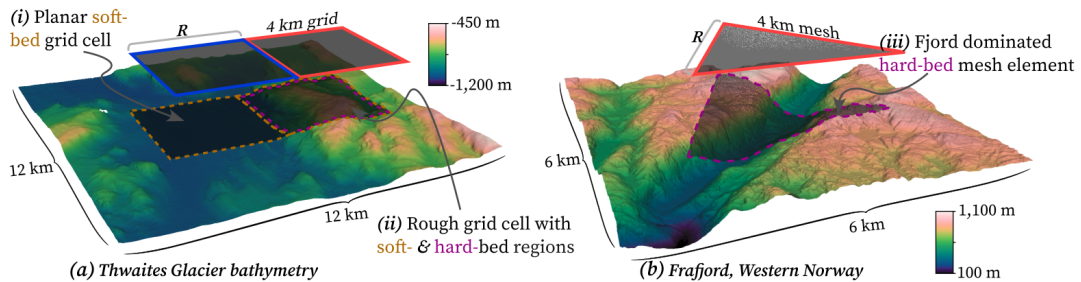


**Fig. 3. Typically sized grid cells and mesh element overlain on previously glaciated regions.** Thwaites Glacier bathymetry is from Hogan and others (2020). Frafjord topography is from Kartverket.no.

we consider if a *simple* (i.e. controlled by a single parameter) unified sliding relationship is a realistic possibility, consider the settings and scales under which Iken's bound may not hold, and make suggestions for the application of sliding relationships to models (Section 6).

Throughout this paper we use *sliding* to refer to the net effect of processes that fall within the 'inner flow' (covered below), and *slip* to refer to discrete slip at the ice-bed interface where a clear ice-bed interface can be discerned. Unless otherwise specified, we refer to sliding situations where the ice-bed interface is at the pressure melting point. We hope that this paper is useful to those seeking an introduction to glacier sliding and coverage of advancements over the last decade, but we do not attempt an exhaustive review. Earlier reviews (Clarke, 2005; Fowler, 2010) and book chapters (Benn and Evans, 2010; Cuffey and Paterson, 2010) provide more comprehensive coverage. Our discussion is limited to continuum-scales in ice and we do not cover crystal-scale deformation or molecular-level interaction – Schulson and Duval (2009) and Krim (1996) provide more information on these topics.

## 2 INNER-OUTER FLOWS

Fowler (1977), Fowler and Larson (1978), and Fowler (1981) (hereafter Fowler1977) consider glacier sliding over a two-dimensional free-slip bumpy bed analytically. Recognising that the smooth basal boundary used in larger-scale analytical models is not a realistic representation of a rough glacier bed, Fowler1977 separate ice motion into an 'inner' flow and an 'outer' flow (reinterpreted in Fig. 5). The inner flow, which includes a component of basal slip, is theorised to closely follow the *actual* bed topography. The outer flow accounts for internal deformation at the typical depth and length scale of the entire glacier and is considered to be 'sliding' over a smoothed representation of the actual bed (i.e. the *model* bed). The outer and inner flows are then joined by a sliding relationship under the condition that the inner flow 'feels' the outer flow as a uniform shearing flow, and the outer flow 'feels' the inner flow as a tangential stress at the smoothed bed boundary.

In our application, the inner flow accounts for the relevant subset of processes outlined in Fig. 4 and Section 3 (as opposed to the simpler set of processes considered in Fowler1977) and the outer flow comprises englacial ice deformation with minimal influence from the processes in Fig. 4. In a modelling sense, the outer flow represents all motion not captured by the basal sliding component. A more complex example of multiple sub-processes operating in an inner flow is given schematically in Fig. A2.

A distinction between an inner and outer flow begins to form an inclusive description of glacier sliding, but a consistent definition for the position of the inner-outer boundary does not immediately materialise – even if an explicit inner-outer boundary is in keeping with its implicit use in previous studies (e.g. Schoof and Clarke, 2008; Zoet and Iverson, 2020; Helanow and others, 2021). The inner flow does not neatly fit the idea of a boundary layer as typically used in fluid dynamics to describe a region of turbulent flow separation (Batchelor, 1967 and discussed further in Section 3.3) and shares only broad similarities with a bottom boundary layer as used in oceanography models (Campin and Goosse, 1999). A numerical approach also means that the inner and outer flow can not be matched analytically as they are in Fowler1977. However, perturbations in strain rates tend to decrease in amplitude with increasing height above the bed, either exponentially (Balise and Raymond, 1985) or as a power-law (Chandler and others, 2006); corresponding length scales for the decay of inner layer strain rate perturbations could then form a basis for defining the inner-outer layer boundary.

The height at which inner-flow processes become negligible will also vary as a function of the spatial scale under consideration, heterogeneity in bed properties, and the roughness characteristics of the bed topography. For example, inner-flow processes will be important at a greater height above the bed if considering an area of rough topography around a planar soft-bed region, than if considering the planar soft-bed region in isolation. In most situations however, a reasonable norm is already defined for setting the position of the model bed surface. BedMachine (Morlighem and others, 2017) and BedMap (Fretwell and others, 2013) products are used for the Greenland and Antarctic ice sheets respectively while a more fragmented approach is taken for mountain glaciers (e.g. Welty and others, 2020; Grab and others, 2021). These bed topography models are significantly smoother than the roughness suggested by geostatistical analysis of radar flight lines (MacKie and others, 2021; Law and others, 2023) and deglaciated forelands immediately adjacent to the ice sheets, but function as convenient thresholds for separating inner and outer flows. Crucially, we note that the imperfect representation inherent to subglacial bed topography products means a degree of ice deformation will unavoidably already be incorporated within existing sliding parameterisations even if its inclusion has not been previously formalised. The error associated with a collapsed inner flow is therefore not introducing new errors, but rather providing a way to quantify and address existing ones.

Using this description of the inner flow, the net basal traction,  $\tau_b$  or  $\boldsymbol{\tau}_b = (\tau_{b,x}, \tau_{b,y})$  for higher-dimensional set-

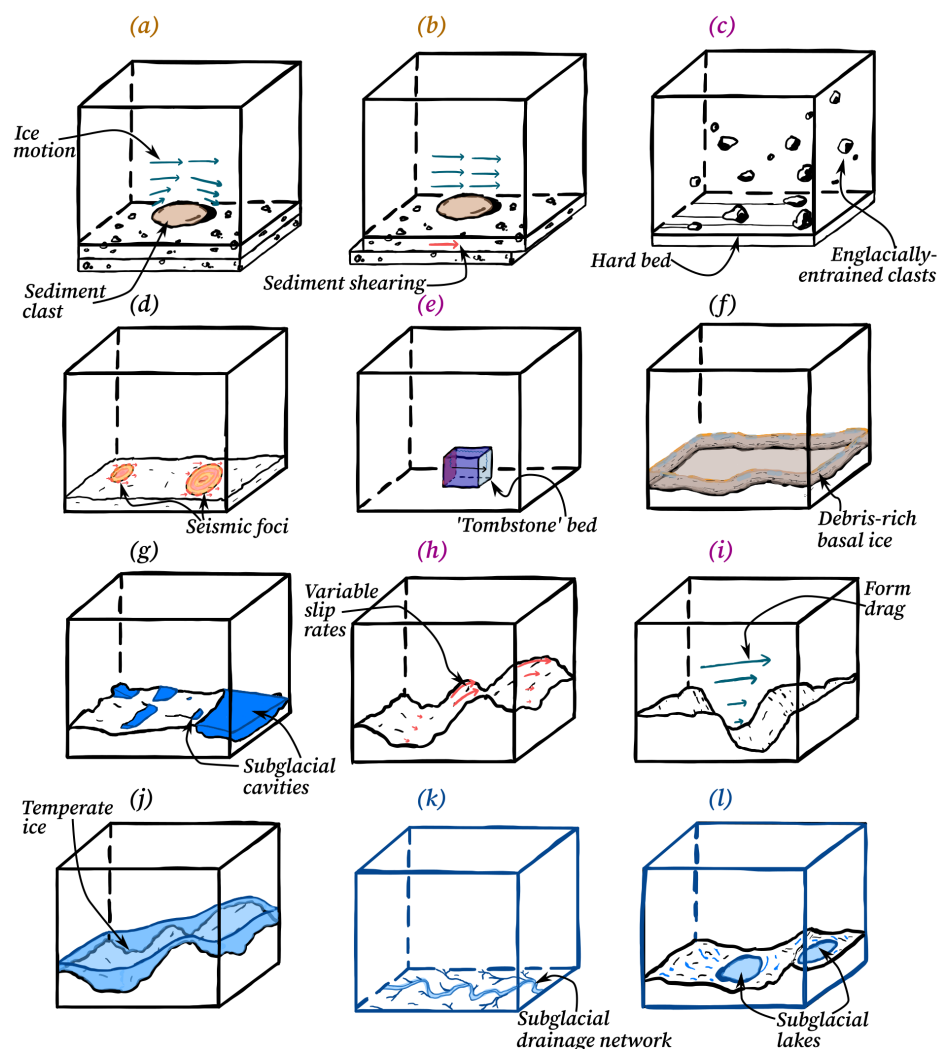


**Fig. 4. Schematics of glacier sliding sub-processes and controls discussed in the text.** Scale is intentionally omitted but scale generally increases left to right and top to bottom through sub-processes. Hydrology in **k** and **l** is considered as a process modifier, as no ice mass is transported and these are distinguished with blue outline boxes. **a** Form drag over sedimentary clasts. **b** Shear of sediment. **c** Ice with clasts sliding over a flat hard bed. **d** Stick-slip events. **e** Regelation. **f** Deformation within the basal boundary layer. **g** Cavitation. **h** Spatially variable sliding rates over rough topography. **i** Spatially variable ice deformation over rough topography. **j** Temperate layer processes. **k** Hydrology and channelisation. **l** Subglacial lakes.

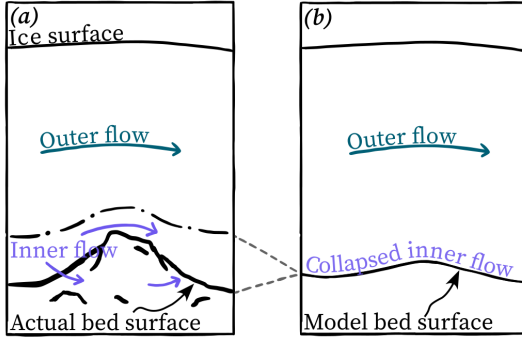


**Fig. 5. Inner and outer flows.** **a** Outer flow and inner flow with matching surface (dash-dot line) which may be similar, but is not directly equivalent, to the model bed surface. Depending on setting the inner flow may feature any of the processes in Fig. 4. **b** The inner flow is collapsed to occur at the model bed surface. The outer flow represents ice deformation that is not significantly influenced by bed processes.

tings, at the model bed surface can then be treated as the sum of multiple individual sliding processes and upslope bed resistance. Here, we separate these processes into traction components for the following categories: resistance to discrete *slip* at the ice-bed interface represented as  $\mathcal{S}$ , resistance to distributed *viscous* deformation within the ice as  $\mathcal{D}$ , and *geometric* resistance to flow from up-slope obstacles as  $\mathcal{G}$ , with each printed in bold font to represent vector components. In a one dimensional case we can relate  $\mathcal{S}$  to the slip velocity at the ice-bed interface,  $u_s$ ,  $\mathcal{D}$  to the velocity between the ice-bed interface and the inner-outer boundary,  $u$ , and  $\mathcal{G}$  to the slope orientation,  $\theta$ , though we remain agnostic about the exact functions tying these terms together for now. Summing these components for a simple one-dimensional case gives

$$\tau_b = \sum_i \mathcal{S}_i(u_s) + \sum_i \mathcal{D}_i(u) + \mathcal{G}_i(\theta) \quad (2)$$

for each sub-process  $i$  within each category.

Considering next a region,  $R$ , that could be taken as a model cell (Fig. 6), and which may contain sliding processes that vary through space, where the plane defined by  $x$  and  $y$  follows the average surface slope,  $\theta$ , over the region. We can then define each sub-process as additionally being a function of space using an indicator function  $I_{R_i}(x, y)$  dependent on a sub-region  $R_i$  where

$$I_{R_i}(x, y) = \begin{cases} 1 & \text{if } (x, y) \in R_i, \\ 0 & \text{otherwise.} \end{cases} \quad (3)$$

with each  $R_i \subseteq R$ . Focussing on traction, this gives a

total,  $\mathcal{S}_T$ , of slip processes as

$$\mathcal{S}_T(x, y, \mathbf{u}_s) = \sum_{i \in \{\alpha, \beta, \gamma, \dots\}} I_{R_i}(x, y) \mathcal{S}_{R_i}(\mathbf{u}_s) \quad (4)$$

where the subscript  $R_i$  refers to a slip process occurring in  $R_\alpha, R_\beta$  and so on (Fig. 6) and  $\mathbf{u}_s = (u_{s,x}, u_{s,y})$  refers to the slip velocity at the ice-bed interface within each  $R_i$  which can be defined using local basis vectors. For practical applications to discretised grid cells  $b_{i0}$  should therefore define a plane. Appendix A1 shows an example of  $\mathcal{S}_T$  expanded into cases for three overlapping regions. This formulation furthermore follows most work on glacier sliding in assuming velocity is continuous in time (i.e. not stick-slip). Similarly for distributed processes

$$\mathcal{D}_T(x, y, \mathbf{u}, b_b, b_{i0}) = \sum_{i \in \{a, b, c, \dots\}} I_{R_i}(x, y) \mathcal{D}_{R_i}(\mathbf{u}, b_b, b_{i0}) \quad (5)$$

where  $b_b$  is the position of the ice-bed interface,  $b_{i0}$  is the position of the inner outer boundary, and  $\mathbf{u} = (u_x, u_y, u_z)$  refers to the velocity field within the zone of deformation considered. For now we remain agnostic about the nature of the functions relating  $\mathcal{S}_T$  and  $\mathcal{D}_T$  to  $\mathbf{u}_s$  and  $\mathbf{u}$  respectively. Geometric resistance is then defined as

$$\mathcal{G}(F_n, \mathbf{n}) = -I_{F_n}(F_n) \begin{pmatrix} F_n \cdot n_x \\ F_n \cdot n_y \end{pmatrix} \quad (6)$$

where  $F_n$  is the normal force at a given point and  $\mathbf{n} = (n_x, n_y, n_z)$  is the corresponding unit normal vector defining the orientation of the ice-bed interface.  $I_{F_n}(F_n)$  is another indicator function defined as

$$I_{F_n}(F_n) = \begin{cases} 1 & \text{if } F_n \geq 0, \\ 0 & \text{if } F_n < 0. \end{cases} \quad (7)$$

used in order to avoid integrating over regions of negative normal force. In practice and at longer (i.e. annual) time scales there should be no persistent negative normal force. If cavities have formed there are two strategies to deal with them under this framework. First, we can assume the cavities are fully developed and take the water-ice interface where  $F_n \approx 0$  as the *de facto* ice-bed interface. The interface between ice and water can then simply be accommodated with a  $\mathcal{S}_{R_i}$  function (Eq. 4) through a frictionless relationship. Second, if  $R$  covers a sufficiently large area, cavitation processes at a small scale can be subsumed within  $\mathcal{S}_T$  as a slip process (e.g. Helanow and others, 2021).  $\mathcal{S}_T$ ,  $\mathcal{D}_T$ , and  $\mathcal{G}$  can then be integrated over  $R$  to provide the area-averaged traction at the model bed interface

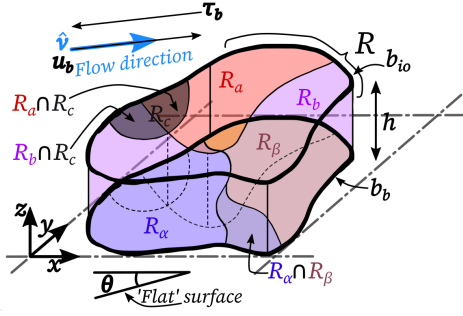


**Fig. 6. Sub-regions related to sub-processes within a given region  $R$ .**  $R_\alpha$  and  $R_\beta$  refer to slip sub-processes (Eq. 4), with the sub-region labelled  $R_\alpha \cap R_\beta$  featuring both  $R_\alpha$  and  $R_\beta$ .  $R_a$ ,  $R_b$ , and  $R_c$  refer to distributed deformation processes (Eq. 5) extend over height  $h$ . Dot-dash lines indicates the possible extension of region  $R$  from a curved shape to a rectangular grid cell. We keep the vertical positions of  $b_b$  and  $b_{io}$  constant in this diagram, but this does not need to be the case.

$$\tau_b|_R = \frac{1}{R} \iint_R (\mathcal{S}_T(x, y, \mathbf{u}_s) + \mathcal{D}_T(x, y, \mathbf{u}) + \mathcal{G}(F_n, n)) dR \quad (8)$$

which could additionally be modified to include e.g. distributed deformation within a sediment layer through an additional term within the double integral.

It is further possible to remedy our agnosticism of the functions relating traction to velocity through the use of generic constitutive relationships for slip and deformation. Setting a given

$$\mathcal{S}_{R_i} = -I_{R_i}(x, y) P_{R_i} \left( \frac{|\mathbf{u}_s|}{|\mathbf{u}_s| + u_{tR_i}} \right)^{\frac{1}{m_{R_i}}} \frac{\mathbf{u}_s}{|\mathbf{u}_s|} \quad (9)$$

where  $P_{R_i}$ , and  $m_{R_i}$ , and  $u_{tR_i}$  are constants for a given region  $R_i$  and which can represent the regularised-Coulomb relationship in Table 1, with the possibility to additionally incorporate  $N$  if it is considered to be fully parametrised within  $P$ , or in a similar manner for a power-law relationship. A generic viscous distributed deformation sub-process can then be

$$\mathcal{D}_{R_i} = -I_{R_i}(x, y) K_{R_i} \int_{b_b}^{b_{io}} \left( \frac{(2\dot{\epsilon}_x)^{\frac{1}{n_{R_i}}}}{(2\dot{\epsilon}_y)^{\frac{1}{n_{R_i}}}} \right) dz \quad (10)$$

where  $b_b$  is the position of the ice-bed interface,  $b_{io}$  is the height of the inner-outer flow boundary (Fig. 6),  $\dot{\epsilon}_x^2 = \dot{\epsilon}_{xi}\dot{\epsilon}_{xi}$  and  $\dot{\epsilon}_y^2 = \dot{\epsilon}_{yi}\dot{\epsilon}_{yi}$  are the effective strain rates in the  $x$  and  $y$  directions respectively, obtained from the strain rate tensor  $\epsilon_{ij} = \frac{1}{2} \left( \frac{\partial u_i}{\partial x_j} + \frac{\partial u_j}{\partial x_i} \right)$ . Similarly to Eq. 9,  $K_{R_i}$  and  $n_{R_i}$

are constants for a given region  $R_i$ , but can be related to the parameters  $A$  and  $n$  respectively in the commonly used Nye-Glen isotropic flow law (Nye, 1952; Glen, 1955),  $\dot{\epsilon} = A\tau_e^{n-1}\tau$ , where  $\tau_e^2 = \frac{1}{2}\text{tr}(\tau^2)$  is the effective stress and  $\tau$  is the deviatoric stress tensor.

It is more challenging to suggest a boilerplate equation for  $\mathcal{G}$ . At very low Reynolds numbers low-angled obstacles provide minimal or negligible resistance, but steep and abrupt obstacles may present important resistance contributions, which cannot be calculated analytically except in special cases (Fox and others, 2006). Usually, the resistance,  $F_D$ , from a single more prominent obstacle is defined as

$$F_D = C_D \frac{1}{2} \rho v^2 A \quad (11)$$

where  $C_D$  is the drag coefficient specific to that obstacle and usually obtained experimentally,  $v$  is the background velocity around the obstacle, and  $A$  is the cross-sectional area of the obstacle opposing flow (Fox and others, 2006, 9.7). We therefore stop short of suggesting an explicit relationship for  $\mathcal{G}$  here, given the uncertainty in its form for potentially complicated bed geometries. Suffice it to say for now that  $\mathcal{G}$  will have negligible importance for very smooth beds, but be an increasing function of velocity, obstacle prominence,  $O_p$ , and obstacle frequency,  $O_f$ , which can be represented functionally as

$$\mathcal{G} = f(\mathbf{u}_b, O_p, O_f). \quad (12)$$

We leave it to future studies to better quantify  $\mathcal{G}$  in the context of realistically rough landscapes, but provide Eq. 12 as scaffolding in the meantime.

Overall, this framework extends from Fowler1977 to include arbitrarily many sub-processes in three dimensions and facilitates quantification of the role of each sub-process in the inner flow, though a full representation will be further complicated in reality; for example if we consider multiple rheological layers between  $z = 0$  and  $z = h$ . Form drag is covered in greater detail later (Section 3.3), but we henceforth intend the sum of  $\mathcal{D}$  and  $\mathcal{G}$  when we refer to form drag processes. We consider how this framework could relate to a unified sliding relationship in Section 6.3.

## 3 SLIDING PROCESSES

### 3.1 Sliding over ‘soft’ (sediment) beds

Early work on soft-bed sliding suggested that subglacial till behaves as a mildly non-linear Bingham viscous fluid (such that resistance to deformation increases with deformation rate), with distributed deformation extending around 50 cm

below the ice-bed interface (Boulton and Hindmarsh, 1987). This idea received some support from contemporaneous studies of subglacial conditions (Blake, 1992; Humphrey and others, 1993) but most subsequent studies – including laboratory, direct measurement, and analogous laboratory experiments from different material science disciplines – find strain localisation close to the ice-bed interface, or manifest in multiple discrete shear zones at multiple depths within the subglacial till, and a Coulomb-plastic rheology (e.g. Biegel and others, 1989; Kamb, 1991; Hooke and others, 1997; Iverson and others, 1997; Iverson and others, 1998; Iverson and Iverson, 2001; Damsgaard and others, 2013; Cuffey and Paterson, 2010), and we therefore do not discuss viscous sediment deformation further.

In laboratory experiments of glacial-till deformation beneath a rigid shear ring, the till reaches its yield strength and then fails at a uniform rate under steady conditions, with a near-constant or a modest decrease in basal traction over a large ( $400 \text{ m a}^{-1}$ ) shear-ring velocity increase (Iverson and others, 1998; Fischer and others, 2001; Iverson, 2010). Field observations using strain-gauges emplaced in actively deforming subglacial sediment repeatedly support Coulomb-plastic deformation (Iverson and others, 1995; Alley and Whillans, 1984; Fischer and others, 2001), with an inverse relationship between pore-water pressure and sediment strength (Fischer and others, 2001). Numerical models indicate that the pore-water pressure-strength relationship is further modulated by till permeability properties (Damsgaard and others, 2017, 2020), with till properties influenced in turn by crushing and compression from overlying ice (Iverson, 1999). Field observations additionally emphasise the importance of ploughing of clasts lodged at the ice-till interface, particularly where sediment pore pressure is high, as the pressure exerted by the clast on the downflow sediment can locally increase the water pressure and weaken the sediment (Iverson and others, 1994; Rousselot and Fischer, 2005). In the case where sediment is not weakened by an increase in pore pressure, a clast may be pushed downwards and no longer be ploughed through the matrix (Clark and Hansel, 1989).

More recently, Zoet and Iverson (2020) used a ring of temperate ice  $\sim 15 \text{ cm}$  thick between the rigid shear ring and underlying sediment. In this setting, rate-strengthening behaviour occurs at lower velocities (below around  $50 \text{ m a}^{-1}$  in sediment with clasts, Fig. 4a) as ice viscously deforms and regelates around static clasts before the clasts begin to plough through the finer-grained matrix at a stress limited by the till's Coulomb strength (Fig. 4b). The net result of the Zoet and Iverson (2020) experiment is a regularised-Coulomb relationship (Fig. 1, Table 1) where the sliding interface is defined up  $15 \text{ cm}$  above the ice-till interface.

Bedforms, including drumlins, mega-scale glacial lineations, and ribbed moraine (Stokes, 2018) are ubiquitous in areas of continuous sediment and likely represent a continuum of features formed by glacier dynamics and subglacial hydrology (Ely and others, 2023). These bedforms are generally streamlined and have a low aspect ratio (height/length), but their contribution to form drag has not been quantified to our knowledge.

### 3.2 Sliding over ‘hard’ (bedrock) beds

Hard-bed sliding studies can be divided into those considering slip across planar surfaces of limited extent and those concerned with sliding over rough or undulating beds at longer wavelengths. In studies considering planar surfaces water pressure is typically kept spatially constant, while in studies considering a rough or undulating bed subglacial water may be theorised as either a microscopically thin and continuous layer, or as a pressurised system of subglacial cavities occupying local bedrock depressions. Undulating beds with a frictionless ice-bed interface were the first to attract attention in sliding theory, but we begin with macroscopically flat (i.e. flat to the naked eye) surfaces due to their simplicity. Roughness at length scales beyond  $25 \text{ m}$  is covered in Section 3.3.

The slip of ice over a planar surface (Fig. 4c) is closer to the assumptions of standard Coulomb behaviour (Coulomb, 1785; Desplanques, 2014), though plane-normal velocity components, englacial clasts, and possible clast-scale cavitation present complications (Hoffman and others, 2022). Rather than a sliding relationship of the form of Eq. 1, basal traction in these studies is often reported as a static  $\mu_s$  or transient  $\mu_t$  coefficient of friction,  $\mu_s$  or  $\mu_t = \frac{\tau_b}{N}$  where  $\mu_s$  describes the force required to move the plane from stationary and  $\mu_t$  describes the force required to keep the plane in motion. Shear-ring studies using temperate ice and englacial sediment content of 0-20% over macroscopically flat granite find a  $\mu_s$  of 0.02-0.05 (Barnes and others, 1971; Zoet and others, 2013; McCarthy and others, 2017; Thompson, 2020), lower than teflon-on-teflon with no lubrication (Fetfatsidis and others, 2013). In the above studies, sliding may be stick-slip or steady-state (outlined further in Section 3.5) depending on water pressure and particular material properties. Transient coefficients of friction between 0.05-0.08 were obtained from subglacial access to the ice-rock interface of the Engabreen outlet glacier in Norway (Iverson and others, 2003; Cohen and others, 2005). Unexpectedly high shear traction values of up to  $0.5 \text{ MPa}$  accompany the low  $\mu_t$  values at Engabreen and these are still not fully explained, suggesting a possible gap in understanding – see Thompson and others (2020) for a more in depth discussion (and note that, in calculations of

transient friction, in contrast to static friction, the line defined by  $\mu_t$  will not necessarily pass through the graph origin of  $N$  and  $\tau_b$ ). The transient coefficient of friction is much higher for cold ice (0.5 at  $-20^\circ\text{C}$ ) making sub-temperate slip very low, but potentially non-negligible (Barnes and others, 1971; McCarthy and others, 2017; Atkins, 2013; Mantelli and others, 2019; Section 3.7).

Where an ice block rests unconstrained on a plane, and water pressure beneath the ice is close to atmospheric pressure,  $\mu_s$  can reach 0.6 for a rough (up to 0.25 cm roughness) pebbly surface or 0.2 for smooth concrete (Budd and others, 1979). These are not typical stress or hydrological conditions for glacier beds (e.g. Hubbard and Nienow, 1997; Woodard and others, 2021) but were used by Budd and others (1979) to derive an empirical sliding relationship (Table 1), with later modifications to exponents to produce a better fit with field data at an ice-sheet scale (Budd and others, 1984) that are arguably large enough to mark a departure from the empirical underpinnings. To summarise planar hard-bed sliding, it is reasonable to treat the friction of ice on rock in the presence of pressurised water as low, but it is not negligible, and may in certain configurations be an important local control on basal traction. There is significant scope to improve understanding in the processes responsible for ice-rock friction across a wide parameter space (Thompson and others, 2020).

Sliding over rough hard beds has also received much attention. This began with the classical work of Weertman (1957), who considered ice motion over isolated cuboids (akin to the geometry in Fig. 4e) with no ice-bed separation through two processes: regelation and enhanced creep (Fig. 4e). In regelation, ice moves without deformation. Temperate ice approaching an obstacle is subject to greater pressure, lowering its melting point. Consequently, some of the ice melts at the upstream face, and the meltwater is driven to the downstream face by the pressure gradient. Here, where the pressure is lower and the melting point is higher, the meltwater refreezes. The higher temperature at the downflow side of the obstacle results in heat flow back through the obstacle, completing the cycle. Regelation is an ongoing process in many subglacial settings (Kamb and Lachapelle, 1964; Kamb, 1970; Hallet and others, 1978; Hubbard and Sharp, 1993; Iverson, 2000; Cook and others, 2011; Rempel and Meyer, 2019), including in soft bed settings outside the scope of the original Weertman (1957) paper. However, the requirement for return heat flow causes regelation rate to vary inversely with obstacle wavelength, limiting the importance of regelation as a sliding process to obstacles smaller than a few cm (Weertman, 1957). Regelation is therefore generally not viewed as a significant contributor to overall sliding rates (MacAyeal, 2019) and has received comparatively little at-

tention since the mid 1990s, though further contemporary study would not be unwelcome.

Enhanced creep is prompted by stress concentrations at bedrock obstacles, leading to locally increased strain rates. Functionally, this means enhanced creep can be considered as a synonym for form drag (Section 3.3), and would fall under  $\mathcal{D}_T$  (Eq. 5) in our framework (Section 2). Conversely to regelation, the contribution of enhanced creep to glacier sliding in Weertman's 1957 study increases with obstacle size. Focusing on the obstacle sizes that produce the greatest rate of sliding when regelation and enhanced creep act in unison (millimetre- to metre-scale) Weertman (1957) reaches a value of  $m$  in a power-law of  $(n + 1)/2 = 2$  with  $C$  representing a combination of bed-geometry characteristics. Technically, values of  $m$  deviating from 2 when  $n = 3$  are therefore not physically based on the original Weertman theory making 'power-law', which we use henceforth, or 'Weertman-type' sliding a more suitable descriptor. Sliding over a sinusoidal two-dimensional bed with no ice-bed separation and a linear ice rheology produces a linear sliding relationship ( $m = 1$  in power-law sliding) (Nye, 1969), as does Weertman sliding with  $n = 1$ .

power-law sliding, usually with  $m = 3$ , is the most commonly used sliding relationship in the latest round of IS-MIP experiments (with linear sliding also frequently used) (Goelzer and others, 2020; Seroussi and others, 2020), yet the theoretical underpinnings supporting these relationships in the original papers do not hold up to scrutiny – including by Weertman's own reappraisal (Weertman, 1979). Weertman's original theory features a non-linear rheology following Glen (1955), but it is apparent that no glacier beds are actually characterised by a controlling obstacle size with the morphology used by Weertman (1957), and even changes to a different unrealistic bed geometry produces a materially different relationship (Lliboutry, 1979). Weertman sliding is further challenged by ubiquitous evidence and theoretical support for subglacial cavitation, or regions of bounded ponded water at high pressure between the glacier sole and underlying hard or soft bed, which form when the pressure on the downstream face of an obstacle falls below a critical level (Fig. 4g and e.g. Walder and Hallet, 1979; Kamb, 1987; Hooke, 1989; Helanow and others, 2021). Weertman sliding also does not provide an explanation for increased sliding rates when subglacial water pressure increases. The persistent utility of power-law sliding in heuristic studies, though generally with  $m \geq 3$ , despite these major problems is covered in Sections 5 and 6.3.

Subglacial cavities (Fig. 4g) act to reduce contact between the glacier sole and the ice bed and may grow as a result of increasing basal velocity or subglacial water pressure.

In the two-dimensional formulations of Lliboutry (1968), Iken (1981), Schoof (2005), and Gagliardini and others (2007), among others, where the bed is comprised of frictionless sinusoids, this produces an upper bound for basal traction, followed by rate-weakening behaviour (Fig. 1). Put mathematically, ‘Iken’s bound’ as coined by Schoof (2005) is given as

$$\tau_b \leq N \tan(\theta) \quad (13)$$

where  $\theta$  is the maximum up-slope angle between the bed and the mean flow direction of the ice (Iken, 1981; Schoof, 2005). Roldan-Blasco and others (2022) suggest that in the simplified two-dimensional framework of compound sinusoids non-negligible friction at the ice-bed interface will not significantly alter the form of the sliding relationship or the existence of Iken’s bound. However, the geometry used in these studies can also be considered unrealistic, with the absence of a third dimension preventing lateral escape of subglacial water which would (1) act to reduce the cavity size (Gimbert and others, 2021) and (2) may place a limit on the maximum obtainable subglacial water pressure averaged over a large region at long (i.e. annual) time scales after the system has had time to equilibrate (e.g. Dow and others, 2015; De Fleurian and others, 2018; Hart and others, 2022). Helanow and others (2019) and Helanow and others (2021) address the three-dimensional problem for smaller scales, and show that realistic three-dimensional bed topographies up to 25 m still result in bounded basal traction, but that significant rate-weakening behaviour is not expected (the regularised-Coulomb relationship in Fig. 1). The validity of the assumptions underlying Eq. 13 when considering inner flows over larger areas and rough topography is covered in Section 6.2.

### 3.3 Roughness, form drag, and temperate ice

Glaciated and deglaciated landscapes are characterised by roughness not only at scales of centimetres to metres (as featured in the previous section), but also by roughness at scales of tens to thousands of metres. This includes cnot-and-lochan landscapes, drumlins, incised fjords, and other erosional or depositional features that bridge a very subjective boundary between ‘roughness’ and ‘topography’ (Figs. 4h-j). Radar flight lines reveal extensive and variably rough beds beneath the Greenland and Antarctic ice sheets (e.g. Bingham and Siegert, 2009; Rippin, 2013; Munevar Garcia and others, 2023), often quantified through a Fast Fourier Transform or variogram (e.g. MacKie and others, 2021) which pares back the geomorphological uniqueness of a landscape but enables regional intercomparison. At present, only roughness up to a length scale of 25 m is explicitly incorporated

in a process-based sliding relationship (Helanow and others, 2021), but it is clear from borehole observations (Ryser and others, 2014; Doyle and others, 2018; Maier and others, 2019; Law and others, 2021) and simulations of ice motion over rough terrain at multi-kilometre scale (Hoffman and others, 2022; Law and others, 2023; Liu and others, 2023) that roughness at larger scales significantly influences patterns of ice motion. Deformation rates are highly variable in proximity to the bed (Fig. 4i) with basal slip ranging between 5%-95% of total surface velocity (Fig. 4h) and much higher slip rates over topographic highs (Law and others, 2023). Existing soft- and hard-bed sliding theories and parameterisations do not incorporate these processes – yet the limited studies that have investigated its influence on bed properties suggest a notable control (Wilkins and others, 2015; Gillet-Chaulet and others, 2016; Falcini and others, 2018).

In polythermal glacier and ice-sheet settings, a layer of lower-viscosity basal temperate ice (Fig. 4j) may furthermore modulate the complex motion patterns caused by topographic roughness (Krabbendam, 2016; Law and others, 2023), with greater thicknesses of temperate ice found in topographic troughs than peaks, and the formation of a shear band at the top of the temperate zone (Law and others, 2023; Liu and others, 2023). The rheology of pure temperate ice has recently been constrained as likely linear viscous (Lliboutry, 1971; Adams and others, 2021; Schohn and others, 2025), though the rheology of temperate ice with a high impurity content remains unconstrained through laboratory experiments to our knowledge.

The influence of roughness on sliding can be theorised through form drag, even if it is at first glance complicated to delineate the transition between ice deformation contributing to presently-derived hard bed sliding relationships (Section 3.2), and ice deformation contributing to form drag. Kyrke-Smith and others (2018) consider the influence of increasing the spatial resolution of a numerical model from 5 km to 0.5 km (and therefore also increasing the fidelity of the underlying topography) on the basal traction obtained from an inversion procedure. Intuitively, Kyrke-Smith and others (2018) find that as spatial resolution is decreased, basal traction increases. Form drag is then described as the area-averaged basal traction with high topographic fidelity subtracted from the area-averaged basal traction with low topographic fidelity, i.e. the basal traction arising from topographic obstacles not explicitly represented by the basal boundary position. This clearly aligns with the idea that form drag can be theorised as part of the inner-flow which collapses to the modelled bed surface (Section 2). At a much smaller scale, Minchew and Joughin (2020b) comment on Zoet and Iverson (2020) and invoke form drag as the viscous

resistance that arises as ice deforms over entrained clast ‘micro-topography’ in laboratory soft-bed sliding experiments before the sediment reaches its yield strength described previously in Section 3.1.

Form drag may therefore be a very useful concept in descriptions of glacier sliding, but its use in glaciology differs fundamentally from form drag as originally described for many aerodynamic applications. The differences are sufficiently large that it may be more appropriate to use a different phrase altogether but we maintain the the phrase ‘form drag’ for continuity with previous studies. In aerodynamic applications, form drag refers to the force acting on a solid body moving through a viscous and locally-turbulent fluid that is opposite and parallel to its velocity and which is not accounted for by induced drag, where the induced drag is a force resulting from turbulent vortices connected to the lift on the body (Batchelor, 1967, sections 5.11, 7.8). Form drag has also been used in atmospheric and ocean dynamics, where it typically refers to the entire drag force resulting from turbulence around an obstacle or obstacles fixed to the surface, rather than a division of it (e.g. Arya, 1973; Renfrew and others, 2019; Jagannathan and others, 2023). Difficulties are still encountered when applying the concept of form drag to settings where there is a fixed continuous surface however, even if turbulence is present (MacCready and others, 2003).

To circumvent the problem of defining form drag only at a specific scale – i.e. for ‘topographic’ roughness (Kyrke-Smith and others, 2018) or for ‘sedimentary-clast’ roughness (Minchew and Joughin, 2020a) – we define form drag here as  $\mathcal{D}_T + \mathcal{G}$ : the sum of all distributed viscous deformation and geometric contributions to the resistive stress operating over a given region within the inner layer. This means deformation processes across a very wide spatial scale (Fig. 2) including temperate ice (this section), basal ice layer processes (Section 3.4), and ‘enhanced creep’ described in the original Weertman (1957) paper are all taken as form drag components under our definition. We make this grouping lacking a consistent rule to meaningfully make distinctions between these processes.

### 3.4 The basal ice layer and ice rheology

A basal ice band of a distinctly different nature to clean meteoric ice, referred to here as the basal ice layer (Figs. 4f, 7), but which may also be called the frozen fringe (Meyer and others, 2018), is frequently a feature of the lowermost section of glaciers and ice sheets. The basal ice layer is characterised by entrained debris and the diagenetic modification (or metamorphism) of meteoric ice by hydrologic processes, melting, refreezing, and intense strain (see Hubbard

and Sharp, 1989; Knight, 1997; Souchez and others, 2000; and Hubbard and others, 2009 for comprehensive reviews). A basal ice layer is observed in deep ice-divide Greenlandic and Antarctic ice sheet ice cores (e.g. Gow and others, 1979; Gow and Meese, 1996; Souchez and others, 1998; Tison and others, 1998; Souchez and others, 2002), Greenlandic and Antarctic ice sheet margins (e.g. Swinzow, 1962; Tison and others, 1993), and across many alpine and ice-cap settings (e.g. Hubbard and Sharp, 1995; Lawson and Kulla, 1978). Proposed formation mechanisms for the basal ice layer are basal freeze on entraining sediment through regelation (at a scale of up to around one meter) (e.g. Weertman, 1961; Hubbard and Sharp, 1993), a pressure-driven heat pump of temperate ice (up to a scale of several meters) (Robin, 1976), or movement of subglacial meltwater along hydro-potential pathways to a region of the glacier bed below the pressure melting point (e.g. Bell and others, 2011). Basal melting associated with frictional heat generated through slip is expected to decrease the thickness of the basal ice layer and impede its growth (Hubbard and Sharp, 1989; Knight, 1997). However, large basal ice layer thicknesses (up to 30 m) are recorded at the western terminus of the GrIS (Fig. 6, Knight and others, 2002) and it is not conclusive if these sequences formed from freeze on in the immediate vicinity of the margin, or survived passage through up to 100 km of thawed bed conditions and slip-driven basal melt (MacGregor and others, 2016). Recent modelling and radar mapping of Antarctica suggests thick (>100 m) sequences of sediment-laden basal ice may persist for tens of kilometres at least beyond a transition from frozen to thawed bed settings (Franke and others, 2024) but further work is required to fully explore the parameter space of these processes. Further, spatially and temporally varying basal ice characteristics ranging from debris-rich ice to frozen sediment, will blur the distinction between soft- and hard-bedded regions.

Shear-ring laboratory experiments for the deformation of a 1-2 cm thick ice-sediment melange between thawed sediments and sediment (Hansen and others, 2024) suggest similar regularised-Coulomb behaviour to shear-ring experiments of clean ice over sediment (Zoet and Iverson, 2020). Meyer and others (2018) also construct an analytical model arguing that ice infiltration into previously thawed sediments limits bed strength (in effect, plastic sliding) in pervasively soft-bedded regions. Beyond these studies however, we are not aware of experiments considering basal ice sequences exceeding a few cm in thickness or the large diversity of facies found in the basal ice layer (Hubbard and others, 2009).

Four further rheological factors present significant complications for ice deformation in the vicinity of the bed and are hence captured at least partially within the inner flow.



**Fig. 7. The basal ice layer at Russel Glacier, Greenland.** From Knight and others (2002) showing characteristic stratigraphy.

First, pre-Holocene ice with a higher dust concentration and typically smaller grain size deposited during the last glacial period deforms at a rate around 2.5 times that of Holocene ice under the same stress and temperature conditions (Paterson, 1991). Such ice is widely present in the strata of the Greenland and Antarctic Ice Sheets (Macgregor and others, 2015; Winter and others, 2019; Ashmore and others, 2020) but uncommon in glaciers and ice caps where it is limited to very slow moving areas (Thompson and others, 1997), though valley glaciers generally feature much higher rates of englacial debris impurities in any case (e.g. Goodsell and others, 2005). Second, ice at depth has a highly anisotropic rheology due to the development of a strong crystallographic preferred orientation under consistent uni-directional deformation (Lile, 1978; Baker, 1981; Duval, 1981; Wilson and Sim, 2002). Such mechanical anisotropy presents major challenges in implementation, bench-marking, and interpretation within numerical modelling (Martín and others, 2004; Gillet-Chaulet and others, 2005) but is nonetheless likely of significant importance within viscous deformation of ice in the inner flow where strain rates are both high and spatially complex (Law and others, 2023). To our knowledge, this aspect of glacier sliding is not covered by any existing glaciological literature. Third, folds close to the bed may arise from mechanical differences in ice layers (Whillans and Jezek, 1987; Bons and others, 2016; Zhang and others, 2023) with the possibility to significantly influence the bulk rheological behaviour of the inner flow. Fourth, while  $n = 3$  is the default in glacier and ice-sheet models (in fact already rounded down from the 3.2 reported in Glen, 1955), there are numerous field-observation based studies suggesting that for cold (i.e. not temperate) ice  $n = 4$ , representing a dislocation creep

regime, is more appropriate in higher stress settings (away from ice-sheet ice divides, for example) (Bons and others, 2018; Millstein and others, 2022; Ranganathan and Minchew, 2024) and perhaps also at areas dominated by pure shear (Gillet-Chaulet and others, 2011). Considering a smooth Bed-Machine lower boundary in northern Greenland,  $n = 4$  dramatically decreases the area over which basal sliding is expected to contribute significantly to total surface displacement (Bons and others, 2018). The influence of  $n = 4$  on form drag and sliding parameterisations, and its interaction with rough topography is to our knowledge entirely unexplored.

Where present, these rheological complications will already be implicitly and unavoidably accounted for via inversion procedures under parameterisations where they are not explicitly accounted for. The potential heterogeneity of their interactions creates significant complexity that future work should seek to disentangle.

### 3.5 Stick-slip and continuous sliding

In most cases, glacier and ice-sheet models neglect acceleration in the Navier-Stokes equations and treat ice as inelastic. These generally reasonable assumptions at typical modelling time-scales require that basal traction and basal velocity are connected through a continuous relationship in the form of Eq. 1 and that rapid (e.g. order of seconds) changes in velocity are not accounted for. However, these requirements are sometimes inconsistent with field observations of sliding, where near-instantaneous stick-slip behaviour (Fig. 4d) is frequently recorded by seismometers and geophones as basal icequakes (e.g. Neave and Savage, 1970; Walter and others, 2013) and also by direct observation at the glacier bed (Theakstone, 1967; Hubbard, 2002). Icequakes are also generated englacially by processes such as extensional faulting near the surface, but these phenomena are not covered here.

Basal icequakes occur due to a rapid release of elastically stored energy, resulting in ice motion that is transiently far higher than the long-term average (Winberry and others, 2009; Podolskiy and Walter, 2016). Moment magnitudes have been recorded from negative in alpine settings (Helmstetter and others, 2015) to magnitude seven at Whillans Ice Stream in West Antarctica (Wiens and others, 2008). For a basal icequake to occur, the local frictional shear strength of the bed must be lower when the sliding interface is in motion than when it is static, i.e.  $\mu_t$  must be lower than  $\mu_s$  (Bahr and Rundle, 1996; Rice and others, 2001) describing slip-weakening behaviour. Stick-slip is usually associated with diurnal or tidal variations in subglacial water pressure allowing a clear build-up period for elastic energy (Bahr and Rundle, 1996; Bindschadler and others, 2003; Walter and others, 2008; Stevens and others, 2024) but basal icequakes

are also recorded outside of such cycles (Hubbard, 2002). Stick-slip behaviour is usually described through a rate-and-state framework (Rice and others, 2001) – as often applied in geological-fault settings (Gomberg and others, 2000; Appendix A3) – where a state variable,  $\psi$ , is introduced to account for the strength of the fault (Rice and others, 2001; van den Ende and others, 2018), usually based on the slip displacement (Ruina, 1983) or its time-dependent evolution (Dieterich, 1979) giving

$$\tau_b = f(u_b, N, \psi) . \quad (14)$$

In contrast to Eq. 1, the expectation is that  $u_b$  in Eq. 14 can vary rapidly in both time and space. A rate-and-state friction relationship can still account for the aseismic rate-strengthening steady slip of a fault (van den Ende and others, 2018) but is not well-suited for models entirely excluding rapid velocity changes and elastic behaviour by design.

Quantifying the contribution of stick-slip basal sliding to glacier motion is challenging due to large uncertainties in fault dimensions, slip displacement, and stress calculated from seismic data (Abercrombie, 2015). Some estimates suggest stick-slip displacement accounts for all basal sliding over an annual period (Helmstetter and others, 2015), while in other cases, coseismic and aseismic regions coexist (Barcheck and others, 2020; Kufner and others, 2021) – analogous to co-existing seismogenic and creeping faults in actively deforming geological faults (e.g. Azzaro and others, 2020).

Despite the growing interest in stick-slip motion in glaciers (e.g. Podolskiy and Walter, 2016; Zoet and others, 2020) there are limited connections between rate-and-state theory (of form Eq. 14) and continuous basal traction theory relationships (of form Eq. 1). We are only aware of the statistical mechanical approach of Bahr and Rundle (1995), where the glacier sole is represented as numerous elastically interconnected blocks with stochastically varying roughness parameters and the similar but simplified 1D approach of (Köpfler and others, 2022). Bahr and Rundle’s approach, intended for thin, steep, valley glaciers, finds that the average total force on an individual block (including elastic forces from adjacent blocks) is proportional to the area-average basal traction,  $\tau_b$ . If this holds for greater ice thicknesses and larger scales then stick-slip behaviour alone will not invalidate continuous basal traction relationships over a sufficiently large grid cell (or representative surface area), but much further work is required to integrate this theory with recent developments in understanding the stick-slip behaviour of glaciers, and how this can relate to the spatial scales of numerical model grid cell resolution.

### 3.6 Overlap between soft- and hard-bed sliding

Most glacier and ice sheet modelling studies use basal traction relationships that implicitly assume the bed is either soft or hard across the entire domain with the ostensibly hard-bed Weertman-type sliding relationship (or equivalently, power-law/pseudo-plastic sliding with  $2 \geq m \geq 4$ ) being the modal choice in ISMIP6 experiments. In some situations a hard-soft division is appropriate, for example most studies are in agreement that extensive, relatively planar sediment lies beneath the ice streams draining into the Ronne and Ross ice shelves in Antarctica (Tulaczyk and others, 2000; Vaughan and others, 2003; Peters and others, 2007), while geographically limited areas of Canadian continental shield may qualify as ‘true’, relatively planar, sediment-free hard beds (Slaymaker and Kovanen, 2017). Many individual valley glaciers can also be reasonably categorised as predominantly soft- (e.g. Murray and Porter, 2001) or hard-bedded (e.g. Hubbard, 2002) (Section ??). However, taking Isunguata Sermia in west Greenland as one well-studied example, borehole data mostly from topographic highs are used to suggest hard-bed conditions are dominant (Harper and others, 2017; Maier and others, 2019) while nearby seismic surveys are used to suggest the opposite (Booth and others, 2012; Dow and others, 2013; Kulesa and others, 2017). Meanwhile, ice-marginal studies in west Greenland (Klint and others, 2013) find a complex mix of bedrock, sediment-filled depressions, and extensive sandurs filling valley bottoms in front of the major land-terminating outlets (Grocott and McCaffrey, 2017). In the case of the seismic survey of Kulesa and others (2017) the recorded seismograms also allow for hard-bed conditions at topographic highs which would be in agreement with Harper and others (2017). Similarly, recent work at Thwaites Glacier in Antarctica further suggests the coexistence of soft- and hard-bed regions over distances less than 10 km (Jordan and others, 2023), supported by distinct along-flow variations in roughness (Holschuh and others, 2020). While soft- or hard-bed categories can be a reasonable distinction for individual glaciers, all available evidence indicates that a more appropriate default for present and palaeo ice-sheets at large is a mixed bed condition vacillating between the two end-members.

Some recent attention has been focused on the interaction between soft- and hard-beds, with Koellner and others (2019) considering 2D flow over sinusoidal beds with wavelengths from 8–60 km and setting the value of  $m$  in the power-law sliding relationship (Table 1) to 8 to approximate regularised-Coulomb sliding in sinusoid troughs, while keeping it at 3 over the sinusoid peaks. This demonstrates that a hybrid  $m = 3 \leftrightarrow 8$  Weertman rheology results in a modelled glacier

response between  $m = 3$  and  $m = 8$  end-members. Given sliding rates at the modelled ice-bed interface can vary significantly over much shorter distances (Law and others, 2023) than considered in Koellner and others (2019), further work is needed to effectively isolate the influence of realistic variations in soft- and hard-bed sliding, and to assess whether hard-bed highs and soft-bed depressions are a reasonable model for the geologic composition of the Greenland and Antarctic ice sheets. Joughin and others (2010) also apply a plastic sliding relationship to inferred soft-bedded regions and power-law sliding with  $m = 3$  to inferred hard-bedded regions Joughin and others (2009) at Pine Island Glacier, Antarctica, finding good agreement in this mixed model over an 8-year period (Section 5).

From empirical studies at small (<25 m) scales, both the derived sliding relationship for hard-bed cavitation (Schoof, 2005; Gagliardini and others, 2007; Helanow and others, 2021) and slip over sediments (Zoet and Iverson, 2020) can yield a bounded traction relationship, leading to suggestions that regularised-Coulomb then represents a ‘universal glacier slip law’ for both hard and soft beds (Minchew and Joughin, 2020b). We cover large-scale remote-sensing/modelling studies which indicate this may not be the case in Section 5, and consider the applicability of a ‘unified’ sliding relationship in Section 6.3, but focus briefly here on the differences that still remain between the regularised-Coulomb sliding relationships of Helanow and others (2021) and Zoet and Iverson (2020). In order to match the relationships of Zoet and Iverson (2020) and Helanow and others (2021) an unrealistically low friction angle is required in the equation of Zoet and Iverson (2020) (Fig. A1), indicating that the set-up of Zoet and Iverson (2020) produces a stronger bed than Helanow and others (2021) under equivalent effective pressure and velocities, despite the general conception that soft beds are weaker than their hard-bed equivalents (e.g. Koellner and others, 2019; Joughin and others, 2009). It is possible that the strength difference is explained by (i) a natural requirement for lower subglacial water pressure in hard beds (by around 4%), which is supported by available evidence (e.g. Engelhardt and others, 1990; Doyle and others, 2018), (ii) non-negligible ice-rock interface friction, which is not included in Helanow and others (2021), or (iii) unaccounted for form drag (i.e. an increase in  $\mathcal{D}_T$  within Eq. 8 if sliding with cavitation described in Helanow and others, 2021, is taken as a process within  $\mathcal{S}_T$ ) occurring in many hard-bed settings which results in a view of a stronger bed.

Last, Tsai and others (2021) take an agnostic approach to the soft- and hard- bed division, focusing instead on the region of the bed where the hydrological system is expected to be active (where  $\tau_b$  is locally set to 0) and inactive (where  $\tau_b$

is locally determined using power-law sliding). Under this formulation Tsai and others (2021) find a relationship similar to Budd and others (1984) sliding (their Eq. 6) which matches well with annual variations in velocity and moulin discharge at a land-terminating sector of the Greenland Ice Sheet. This relationship may be well-applicable in large-scale models (Section 6.3).

### 3.7 Frozen-thawed transitions and sub-temperate sliding

In some simpler theories both sliding and slip are considered to be negligible for frozen beds (Lliboutry, 1966; Cuffey and Paterson, 2010, 7.1.1), but most models either simply neglect a temperature control on sliding (including all models inverting for basal traction with present-day velocity fields in IS-MIP6 experiments) or take a heuristic approach to scaling basal traction with temperature to avoid a stress singularity at the frozen thawed boundary (e.g. Fowler and Larson, 1978; Tarasov and Peltier, 2007; Mantelli and others, 2019) giving

$$\tau_b = f(u_b, N, T_h) \quad (15)$$

as an adaptation of Eq. 1 where  $T_h = T_b - T_{pmp}$  is the homologous temperature calculated from the pressure melting point,  $T_{pmp}$ , and ice temperature at the base,  $T_b$ . This corroborates with field studies finding slow (<0.2 m a<sup>-1</sup>) slip rates even with temperatures some degrees below freezing for both soft- and hard-bed settings (Hallet and others, 1986; Echelmeyer and Zhongxiang, 1987; Cuffey and others, 1999; Fitzsimons and others, 1999). The mechanical process or processes responsible for sub-temperate sliding in these instances remains uncertain (Cuffey and Paterson, 2010, 7.2.8) but may be related to a very thin (nm) premelt layer at the ice bed (Shreve, 1984), the inclusion of solid friction (Fowler, 1986; Section 3.2), or sediment deformation despite freezing conditions Waller (2001). Separately, both form drag and geometric resistance will still be expected under freezing bed conditions, though at a slower rate than under equivalent stress conditions in colder ice. This processes is framed by Weertman (1967) as the continuation of enhanced creep despite the cessation of regelation, and matches Eq. 8 with an absent or much reduced  $\mathcal{S}_T$  component. Expanding sub-temperate sliding out to a grid cell under consideration also allows for the situation of both freezing and thawed areas within the same grid cell (Fig. 8), which may be a common situation in frozen-thawed transition zones (e.g. Oswald and Gogineni, 2012; Dawson and others, 2024). Generally, a pattern of greater basal traction in interior ice-sheet regions where a frozen bed is considered more likely is ob-

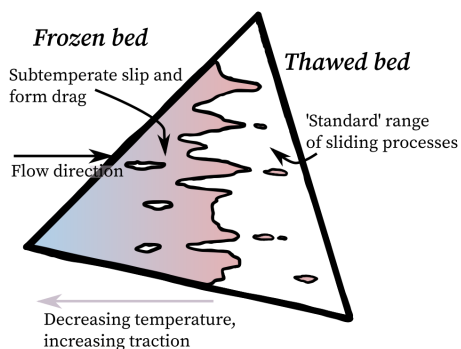


**Fig. 8. Subtemperate sliding.** Triangle represents area  $R$  under consideration. Solid black line represents frozen-thawed transition at the bed and cooler colours represent decreasing temperature of frozen portion of bed. Sub-temperate sliding is not sufficiently well-studied to provide a definite spatial range, but speculatively this may range from 100 m - 10 km. Adapted from Wilch and Hughes (2000).

tained in ice-sheet wide inversions (Larour and others, 2012; Morlighem and others, 2013).

#### 4 SUBGLACIAL HYDROLOGY

Subglacial hydrology and basal sliding are intimately linked via close feedbacks in many glacial settings, with water pressure influencing sliding velocity via the effective pressure  $N$  and sliding velocity in turn influencing  $N$  as changes in cavitation affect hydraulic conductivity and drainage system connectivity (e.g. Schoof, 2010). There are too many facets of this topic to cover comprehensively here (reviews include: Irvine-Fynn and others, 2011; Ashmore and Bingham, 2014; Chu, 2014; Siegert and others, 2016; Nienow and others, 2017; Davison and others, 2019), so we focus briefly on the importance of a spatio-temporally varying subglacial hydrology system, without considering the mechanisms themselves in detail.

In most numerical ice sheet and glacier models, subglacial hydrology is either absent or is parametrised in a simple fashion through the effective pressure  $N$  term in the sliding relationship (Table 1, Fig. 9) – with at least three materially different ways of including  $N$  in Eq. 1 (Table 1). While in the physical sense the meaning of  $N$  as subglacial water pressure subtracted from the overburden pressure at a point in time and space is very clear, its meaning, and ways of quantifying a representative  $N$  at a given scale are not straight forward in a modelling sense. Subglacial hydrological environments are very spatially diverse even at scales of tens of metres, with various terms (e.g. ‘channelised; dis-

tributed; partly-connected’) referring to various end members in a continuum of characteristics (e.g. Hubbard and Nienow, 1997; Hoffman and others, 2016; Rada and Schoof, 2018). Borehole observations and investigations of deglaciated terrains (Fig. 9) evidence this complexity, with widely varying  $p_w$  time series observed in adjacent boreholes (Doyle and others, 2018; Rada and Schoof, 2018; Doyle and others, 2021) capturing distinctly separate components of subglacial hydrology, consistent with theoretical studies finding low-pressure conduits adjacent to higher-pressure regions with reduced hydrological connectivity (Engelhardt and Kamb, 1997; Hewitt and others, 2018). Therefore, while the influence of  $N$  is fairly well understood for specific sliding sub-processes in isolation – for example, cavitation over a relatively flat bedrock area (Helanow and others, 2021), and sediment shearing in a laboratory setting (e.g. Iverson and others, 1998) or through a numerical continuum model (e.g. Damsgaard and others, 2020) – it remains to fully quantify the influence of a spatially variable  $N$  within a given model grid cell. We are so far only aware of the study of Tsai and others (2021) which locally sets  $\tau_b$  to zero over an area considered to be comprised of cavities, or otherwise calculates it following a power-law relationship, resulting in a relationship that overall shares similarities with the Budd and Jacka (1989) sliding relationship (Table 1).

Beyond this, it is challenging to know exactly how to relate  $N$  to other parameters and variables within a standard sliding relationship. In our framework (Section 2), varying  $N$  could be incorporated within the parameter  $P_{R_i}$  in Eq. 9 or power-law equivalent, though calculating its actual spatial distribution would still remain a major challenge. Most extant cases implement a simple linear multiplication (e.g. Choi and others, 2022), but what, for example, if the traction within a region with low  $N$  for a large proportion of its area was actually controlled by a small prominent pinning-point with high  $N$ ?

Moreover, subglacial drainage systems are also observed to evolve diurnally and seasonally in response to supraglacial melt water inputs (Hubbard and Nienow, 1997), even beneath ice ca. 1 km thick (Chandler and others, 2013). This evolution in turn leads to diurnal and seasonal variability in sliding (Willis, 1995; Zwally and others, 2002; Bartholomew and others, 2011; Nienow and others, 2017). Such temporal variability in  $N$  is by design not captured by ice sheet or glacier models employing temporally constant parameters for the basal traction relationship. However, despite the clear importance of subglacial hydrology as a control on sliding at sub-annual scales however, and with the exception of surging glaciers (Sevestre and Benn, 2015), its overall influence on long-term glacier and ice sheet evolution re-

mains debated, particularly with respect to future changes of the Greenland Ice Sheet (e.g. Tedstone and others, 2015; Doyle and others, 2015; Beckmann and Winkelmann, 2023), with major and sustained changes in glacier and ice-sheet velocity fields typically linked to geometry changes rather than intrinsic changes in the hydrological system (e.g. Vincent and others, 2012; Habermann and others, 2013; Moon and others, 2014; Cook and others, 2016; Seroussi and others, 2017; Catania and others, 2018; Dehecq and others, 2018; Gimbert and others, 2021; Frank and others, 2022). However, large-scale observations do indicate that major changes in the hydrological system – such as a switch from marine-terminating to land-terminating outlet glaciers, or an advancement of the ablation zone – may influence large-scale geometry and velocity patterns over a multi-annual timescale (Maier and others, 2022). Subglacial water pressure also plays a crucial control at marine-terminating outlet glaciers grounded below sea level, which we do not cover in detail here, where very low inferred basal traction values and subglacial water pressure very close to overburden make systems particularly susceptible to changes in  $N$  (e.g. Katz and Worster, 2010; Stearns and Van Der Veen, 2018; Minchew and others, 2019; Bradley and Hewitt, 2024).

## 5 HEURISTIC STUDIES

A separate approach to investigating glacier sliding is to use large-scale remotely sensed or field data to heuristically (i.e. through process-agnostic iterative experimentation and adjustment) determine the form of the sliding relationship, which may then be compared to theoretical expectations (Section 3, Table 1). A time series with significant variation in surface geometry is best suited to the decadal time scales over which mass loss is most often considered (Gillet-Chaulet and others, 2016; Gilbert and others, 2023), but several other variations have been exploited (Table 2). Considered in their entirety, these studies indicate that variation in the form of the sliding relationship across variable glacier settings is not readily captured by a single tunable coefficient,  $C$ , obtained through a standard inversion procedure. For example, Gimbert and others (2021) and Gilbert and others (2023) find  $m = 3.1 \pm 0.3$  in power-law sliding for Argentière Glacier in the French Alps using a combination of surface velocity changes, length changes, and direct sliding measurements while Gillet-Chaulet and others (2016) find  $m \leq 5$  and up to 50 well reproduces surface velocities at Pine Island Glacier, Antarctica. Maier and others (2021) meanwhile indicate that a single  $m$  value, also for power-law sliding, cannot be applied to the entire Greenland Ice Sheet with, for example, an  $m$  of 8 in northeast Greenland contrasting an  $m$  of 4 in

central southwest Greenland. Note that in standard applications using power-law sliding,  $C$  is the subject of the inversion and varies in space, while  $m$  is kept constant.

Such studies offer a testing ground for proving the efficacy of a given sliding relationship, but it is important to note that a match to a given theory does not on its own demonstrate that the physical processes that build it up are actually occurring in the study location. This is straightforward in the case of  $m \leq 5$  from Gillet-Chaulet and others (2016) at Pine Island Glacier. No existing theory postulates this relationship (Section 3) so the utility of  $m \leq 5$  in power-law sliding comes either from the fact that it emulates regularised-Coulomb sliding that does have a large body of theory behind it, or it represents a hitherto unappreciated set of processes not presently incorporated into a process-based sliding relationship. Meanwhile, it is difficult to interpret the findings of Minchew and others (2016) from a setting known to have significant till coverage (Björnsson and others, 2003) as anything other than plastic deformation of till. In contrast, Gimbert and others (2021) and Gilbert and others (2023) suggest that their findings of  $m \sim 3$  reflects only the ice deformation component of the original Weertman (1957) paper without the regelation component where  $m = 1$ , neglecting the fact that the original Weertman theory is somewhat dependent upon a combination of both regelation and ice deformation, and not making an allowance for the slip component actively observed beneath Argentière (Vincent and Moreau, 2016; Gimbert and others, 2021). Maier and others (2021) also invoke *Weertman-type* hard-bed physics as justification for lower values of  $m$ , despite the fundamental issues underlying the theory (Section 3.2) and the fact that no theory building upon Weertman (1957), or the original study, presently provide a physical justification for  $n = 4$  or above.

Taken collectively, heuristic studies emphasise a heterogeneity between settings that is not easily reconciled with a single sliding relationship controlled by a single tunable parameter. However, they also present perhaps the most definitive method of accurately determining the optimum sliding relationship for a given modelling setting. A standardised methodology that can be efficiently applied to varying settings utilizing increasingly long datasets could therefore be of use in transparently tailoring sliding relationships for given modelling applications.

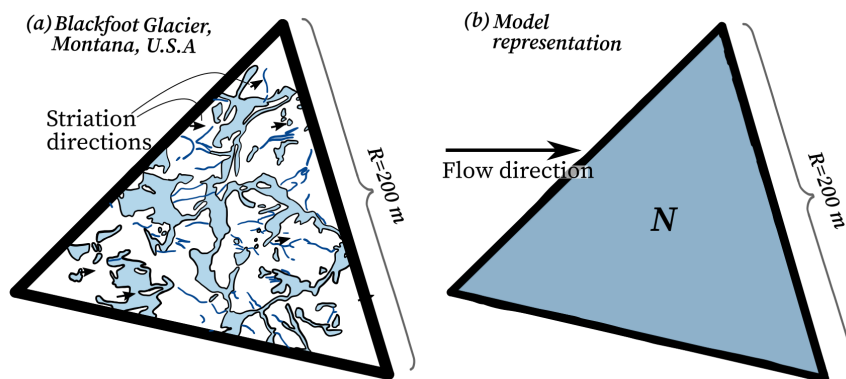


**Fig. 9. Subglacial hydrology as observed in the field or represented in an ice flow model element.** **a** Cavities (pale blue), channels (dark blue lines) and striation flow markers from fieldwork at Blackfoot Glacier (Walder and Hallet, 1979). **b** Simplification to a single mesh element.

| Setting   | Variation  | Study                            | $m$                            |
|---|--|----------------------------------|--------------------------------|
| Argentière, French Alps – valley glacier <sup>‡</sup> | Length (velocity) over 100 (15) years to ~ 2020            | Gilbert and others (2023)        | 3                              |
| Hofsjökull, Iceland – ice cap <sup>§</sup>            | Summer-winter velocity comparison                          | Minchew and others (2016)        | $\infty$ /plastic              |
| Greenland Ice Sheet – ice sheet                       | Single velocity field averaged 2005-2015                   | Maier and others (2021)          | 3-10                           |
| Northwest Greenland – outlet glaciers                 | Forward modelling of mass loss 2007-2018                   | Choi and others (2022)           | 6 in modified Budd             |
| Northeast Greenland Ice Stream – ice stream           | Forward modelling of mass change 2006-2021                 | Khan and others (2022)           | Regularised-Coulomb            |
| Western Greenland – land-terminating outlet glacier   | Annual velocity and hydrology variations 2006-2013         | Tsai and others (2021)           | 4 in modified Budd             |
| Pine Island Glacier, Antarctica – outlet glacier      | Geometry 2003-2008   | Joughin and others (2010)        | mix of 3 and $\infty$ /plastic |
| Pine Island Glacier, Antarctica – outlet glacier      | Velocity in 1996 and 2007-2010                             | Gillet-Chaulet and others (2016) | $\geq 5$                       |
| Pine Island Glacier, Antarctica – outlet glacier      | Forward modelling of velocity field and geometry 2002-2017 | Jouvet and Huss (2019)           | Regularised-Coulomb            |
| Rutford Ice Stream, Antarctica – ice stream           | Displacement over fortnightly tidal cycles                 | Gudmundsson (2011)               | 3                              |
| High Mountain Asia – valley glaciers                  | Velocity fields 2000-2017                                  | Dehecq and others (2018)         | 4                              |
| West Greenland – outlet glacier                       | Front position from 1985-2019                              | Jager and others (2024)          | Regularised-Coulomb            |

**Table 2. Heuristic studies on sliding parameters.** <sup>‡</sup> indicates largely hard bed, <sup>§</sup> indicates largely soft bed. Absence of a superscript indicates ambiguous or mixed conditions. **Notes:** Gudmundsson (2011) did not test  $m$  values above 3. Dehecq and others (2018) combine ice deformation and sliding in a 1D model. Choi and others (2022) also include the influence of  $N$ , defined as ice pressure above hydrostatic equilibrium with a sheet perfectly connected to the ocean, finding best fitting with  $N$  included.

## 6 DISCUSSION

### 6.1 Applying an inner-outer flow framework to multiple sub-processes: bridging hard and soft beds and highlighting the importance of topographic roughness

We can separate the sub-processes covered in Section 3 that deal with continuous, rather than stick-slip, into the three categories defined for Eq. 8. All soft-bed processes and hard-bed processes over macroscopically flat surfaces (Sections 3.1, 3.2) can be defined as slip processes (within  $\mathcal{S}_T$ ). All processes concerning viscous deformation of ice (be it cold, the basal ice layer, or temperate) can be defined as viscous deformation processes (within  $\mathcal{D}_T$ ). Hard-bed sliding processes involving ice deformation straddle slip, deformation, and geometric resistance. The most precise way to include these would be to deconstruct their components (i.e. free slip at the ice-bed interface and over cavities, geometric resistance from obstacles, enhanced deformation) and reimpose them as segregated sub-processes, but this would then place the onus of calculating their evolution with increasing  $u_b$  on each usage rather than allowing for it to be more simply sub-parametrised. This creates particular complications for cavitation, which is very computationally expensive to simulate (Helanow and others, 2021). For the purposes of this discussion we therefore treat ostensibly ‘hard-bedded’ power-law and regularised-Coulomb theories (Section 3.2) as slip processes within  $\mathcal{S}_T$ . This involves the explicit assumption that the region  $R$  is then considered as sufficiently large so as to accommodate topographic features larger than those in Helanow and others (2021), if present.

The relative balance of  $\mathcal{S}_T$ ,  $\mathcal{D}_T$ , and  $\mathcal{G}$  within Eq. 8 then allows us to make assessments of their influence on the overall traction at the inner-outer boundary for a given setting at the scale of ice-sheet or glacier model discretisation. If, as appears reasonable for relatively smooth isolated bed sub-sections (Section 3.6), regularised-Coulomb can represent slip over both soft and hard beds in the presence of abundant meltwater, the term  $\mathcal{S}_T$  becomes agnostic over whether the bed is soft or hard. Then, if the region is relatively planar and  $b_{i0} - b_b$  is relatively small,  $\mathcal{S}_T$  dominates and it is most likely that a regularised-Coulomb relationship emerges. However, if  $\mathcal{D}_T$  (determined as a power-law, Eq. 10) and  $\mathcal{S}_T$  (related to increasing velocity, obstacle prominence, and obstacle frequency, Eq. 12) dominate, then the traction for the given region will be better represented through a power-law. This implies that bed roughness, not bed type is the crucial control on the form of the sliding relationship.

The case of frozen-bed sliding would furthermore shut off, or greatly reduce the importance of  $\mathcal{S}_T$ , resulting in power-law sliding regardless of the roughness characteristics of the region in consideration.

### 6.2 Maximum cavitation sizes, and revisiting Iken’s bound

Bounded sliding relationships involving hard beds are based on the premise that cavities can expand to essentially flood the region considered. In two dimensions this results in rate-weakening behaviour after a maximum point (Schoof, 2005; Gagliardini and others, 2007), while in three-dimensions over realistic small-scale (<25 m) topography the maximum traction is sustained as  $u_b$  increases, with  $\gtrsim 50\%$  of the bed flooded by cavities in a mature system (Helanow and others, 2021). However, cavitation studies generally do not insinuate cavities larger than around 15 m (e.g. Vivian and Bocquet, 1973; Walder and Hallet, 1979; Helanow and others, 2021) and as scales increase subglacial cavities essentially grade into subglacial lakes. Bowling and others (2019) find few lakes exceeding 4 km in size for the Greenland Ice Sheet, with most of these located away from regions of fast motion, giving an estimated total lake coverage of 1.6% of the ice sheet bed. And, while the Antarctic Ice Sheet covers the  $\sim 10,000$  km<sup>2</sup> Lake Vostok (Leitchenkov and others, 2016), it may have an even lower overall lake coverage of <1% (Goeller and others, 2016). Consideration of deglaciated topography, for example near Hardangerfjord in western Norway (Fig. 10), implies multiple instances of areas of steep topography that would not be covered by cavitation, but which would also not be included in bed topography products if they were still covered by thick ice.

If large topographic obstacles are present, such as those in Fig. 10, but large-scale cavities are not concomitant (Fig. A3), then the given grid cell area may come to be dominated by topographic roughness rather than having cavitation essentially smooth over the ice-bed interface (Fig. A3). As discussed in Section 6.1, the stage is then set for the traction defined at the inner-outer boundary to be dominated by resistance related to viscous deformation ( $\mathcal{D}$ ) and bed geometry ( $\mathcal{G}$ ), producing a power-law, rather than a bounded basal traction relationship overall. Nonetheless, while we can place common-sense limits on cavity size in deglaciated areas, a full understanding of the scale distribution of cavities, and its bearing upon Iken’s bound, is an important future research goal.

In addition, Iken’s bound (Eq. 13) is also reliant on the small angle approximation for  $\tan$ , and is therefore not physically meaningful in the situation of steeply oriented cliff faces, as seen pervasively in Fig. 10 and in many rough deglaciated

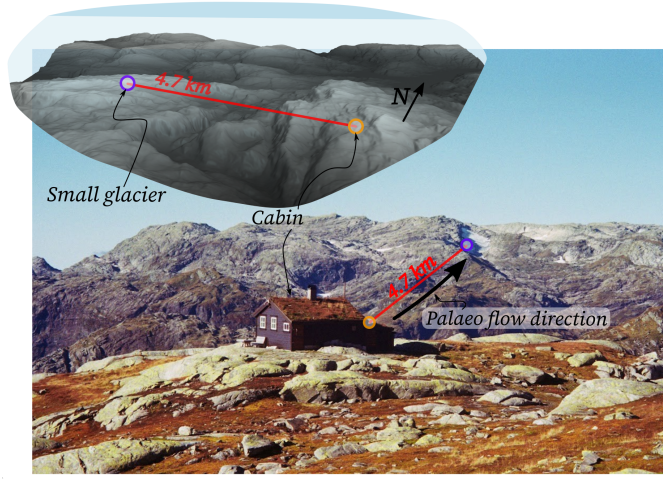


**Fig. 10.** Rough topography near Hardangerfjord, western Norway. Hut location is 60.4526 N, 6.1406 E, inset shows ArcticDEM topography for the valley between the hut and the small glacier in the distance with no vertical exaggeration (Porter and others, 2018). Palaeo flow direction available from e.g. Mangerud and others (2019); Jungdal-Olesen and others (2024). Numerous very steep surfaces opposing the direction of palaeo ice sheet motion can be seen at both a micro and macro scale. Photo taken by RL in late September 2024.

landscapes. We suggest that the unsuitability of Iken's bound in regions featuring steep slopes, coupled with the importance of large topographic obstacles in increasing the  $\mathcal{D}_T$  and  $\mathcal{G}$  terms in Eq. (8) at larger scales may explain the continued efficacy of a power-law sliding relationships in ice-sheet and glacier settings (Table 2).

### 6.3 Does a unified basal sliding relationship exist?

A defining objective of much research into sliding is to uncover a 'universal' sliding relationship which can provide an accurate description of sliding processes across all settings, scales, and time periods. Generally, the implicit assumption is that this will be controlled by a single tunable coefficient (henceforth single coefficient) and/or calculated subglacial water pressure (e.g. Minchew and Joughin, 2020b). Unfortunately, while it may be possible to describe glacier sliding by incorporating a multitude of stress contributions (Eq. 8) the complex nature of myriad sliding sub-processes and their scale and setting dependence (Section 3) likely precludes a single-coefficient relationship applicable to all settings – an outlook supported by the diversity of optimum single-coefficient relationships in Table 2. Instead, the studies reviewed here and Eq. 8 point towards a compound rela-

tionship that bears closer resemblance to descriptions of ice strain comprising several deformation mechanisms (e.g. Eq. 3 of Goldsby and Kohlstedt, 2001).

Nonetheless, we may be able to talk about the general nature of such a compound relationship if, as in Section 6.1, we take regularised-Coulomb (Eq. 9) as the only constitutive relationship for  $\mathcal{S}_T$ , and then take Eq. 10 as the only constitutive relationship for  $\mathcal{D}_T$ . This allows us to take  $\mathcal{S}_T$  and  $\mathcal{D}_T$  as single terms, rather than sums as

$$\mathcal{S}_{T_a} = \frac{-P_{R_r}}{R} \iint_R \left( \left( \frac{|\mathbf{u}_s|}{|\mathbf{u}_s| + u_{tR_r}} \right)^{\frac{1}{m_{R_r}}} \frac{\mathbf{u}_s}{|\mathbf{u}_s|} \right) dR \quad (16)$$

and

$$\mathcal{D}_{T_a} = \frac{-K_{R_r}}{R} \iint_R \left( \int_{b_b}^{b_{i_o}} \left( \frac{2\hat{\epsilon}_x}{(2\hat{\epsilon}_y)^{\frac{1}{n_{R_r}}}} \right) dz \right) dR \quad (17)$$

where the subscript  $T_a$  refers to total aggregate  $P_{R_r}$ , and  $u_{tR_r}$ ,  $m_{R_r}$ ,  $n_{R_r}$ , and  $K_{R_r}$  are the representative parameters for the given region and which can be defined as e.g.

$$P_{R_r}(x, y) = \frac{1}{R} \sum_{i \in \{\alpha, \beta, \gamma, \dots\}} I_{R_i}(x, y) P_{R_i} \quad (18)$$

for  $P_{R_r}$ . Keeping the definition for  $\mathcal{G}$ , but integrating over  $R$  gives

$$\mathcal{G}_a = \frac{1}{R} \iint_R f(\mathbf{u}_b, O_p, O_f) dR \quad (19)$$

where  $\mathcal{G}_a$  refers to the aggregate geometric resistance.

If we assume that each  $\mathcal{G}_a$ ,  $\mathcal{S}_{T_a}$ ,  $\mathcal{D}_{T_a}$  then defines a representative traction component at each coordinate following a moving window average, rather than for within a specific region, and with an  $R$  size that at least approaches a representative surface element (Section 1), we can set

$$\boldsymbol{\tau}_b = \mathcal{S}_{T_a} + \mathcal{D}_{T_a} + \mathcal{G}_a \quad (20)$$

which can be controlled by a total of 8 parameters (though dependent on the exact nature of the function used to describe  $\mathcal{G}_a$ ). Further, in the condition that the poorly constrained  $\mathcal{G}_a$  does not dominate  $\boldsymbol{\tau}_b$  in a complicated manner, and following the other assumptions in this section, we can say that  $\boldsymbol{\tau}_b$  should always be defined as no more than the sum of a regularised-Coulomb and power-law relationship. For the one-dimensional case aligning with Table 1 that is

$$\tau_b = f_{rC}(u_b) + f_{pl}(u_b) \quad (21)$$

where  $f_{rC}(u_b)$  represents regularised-Coulomb sliding of the form Eq. 16 and  $f_{pI}(u_b)$  is a power-law of the form Eq. 17. Effective pressure may be implicitly included in Eqs. 20, 21 through parameters in  $\mathcal{S}_{T_a}$  and  $f_{rC}(u_b)$  but is presently missing as an explicit parameter. Improved understanding of  $\mathcal{G}_a$  would allow improved confidence regarding the applicability of Eq. 21.

However, as standard inversion procedures are not well-suited to determining multiple parameters simultaneously (Morlighem and others, 2010) and as a compound sliding relationship would complicate implementation, the choice between a compound friction law (e.g. Eq. 20) and single-term equation from Table 1 becomes a compromise between a more realistic representation of friction and a less practical numerical implementation. It may therefore be more appropriate to select a flexible yet simple equation as a sliding relationship which is capable of representing a wide range of behaviours.

#### 6.4 Threshold velocities for regularised-Coulomb sliding

In power-law sliding, two parameters ( $C$  and  $m$ ) control the relationship, but even in the simplest regularised-Coulomb relationship at least one further parameter is required ( $u_t$  in our usage in Table 1) to set the transition point to bounded traction. Laboratory experiments over sediment indicate a transition to bounded traction occurs at around  $50 \text{ m a}^{-1}$  (Zoet and Iverson, 2020) in a controlled setting, while the transition for cavitation over hard beds at small scales ( $<25 \text{ m}$ ) is more variable, and possibly as low as  $5 \text{ m a}^{-1}$  (Helanow and others, 2021). Given that uniformly smooth soft beds of consistent material properties, or hard beds of consistent geometry, are somewhat unlikely, it becomes complicated to suggest a reasonable physically based  $u_t$  value that can be universally applied. For example, Joughin and others (2019) set a threshold velocity of  $300 \text{ m a}^{-1}$  for Pine Island Glacier, Antarctica which sets a clear spatial boundary for the region of bounded traction, but without process-based reasoning for the threshold velocity value. This may be appropriate for the Pine Island setting, but it's not clear if a  $300 \text{ m a}^{-1}$  limit would be equally effective in, for example, rough regions of the Greenland Ice Sheet. As bounded traction significantly increases the sensitivity of outlet glaciers to climate forcing (Ritz and others, 2015; Tsai and others, 2015; Brondex and others, 2019), further work determining the factors controlling the threshold velocity (Trevers and others, 2024) is necessary. We further note that in marine-terminating settings it may be difficult to distinguish whether the  $u_t$  value used results in a good match with observations because of an intrinsic switch in processes beyond the threshold veloc-

ity, or as a result of the increasing influence of the ocean on subglacial hydrology, with ice velocity acting as a proxy for proximity to the coast.

#### 6.5 Which basal sliding relationship to use?

No single extant sliding relationship accounts for the full breadth of processes or observations that comprise glacier and ice-sheet sliding (Sections 3, 5), making it challenging to recommend a single-tunable-coefficient sliding relationship. Pending future investigations, we make the following suggestions based primarily on heuristic studies (Section 5), whose empirically-validated nature makes them more suitable for application to glacier and ice-sheet models.

We suggest that power-law sliding (or equivalently, pseudo-plastic, Weertman-*type* sliding), with a setting-dependent  $m$ , presents a reasonable first choice. Given information from the limited number of studies available (Table 2), and in broad agreement with our discussion (Sections 6.1-6.3), lower  $m$  values ( $\leq 4$ ) are then better suited for rougher settings while higher  $m$  values ( $\geq 5$ ) are better suited for regions where topography is expected or known to be extensively smooth. Therefore, while  $C$  is the main object of the inversion procedure,  $m$  may be assigned based on additional constraints, such as topographic roughness. While we do not doubt the efficacy of regularised-Coulomb in some settings (Table 2), it is simpler to manipulate a power-law relationship to approximate regularised-Coulomb using a high value of  $m$  than vice-versa. As models for glaciers or ice sheets frequently invert for traction coefficients over regions of inferred frozen beds (Goelzer and others, 2020; Seroussi and others, 2020), it is further likely that a regularised-Coulomb relationship would misrepresent these areas.

If hydrology is incorporated, the simplified implementation of Budd sliding as used in Choi and others (2022) and set as the default for ISSM (Larour and others, 2012), which is functionally the same as power-law sliding but with  $N$  included as a multiplication factor is a good starting point. A simplified hydrological model as used in Choi and others (2022) based on elevation above sea level may then be reasonable over annual timescales (Section 4), though we stress that this is an extremely pressing area for future research – as is the exact way in which  $N$  should be incorporated.

##### 6.5.1 A note on terminology

We hope that this paper provides a clear description of the inner flow sub-processes that a sliding relationship will account for under ideal circumstances, and may also ease some of the angst experienced by modelling practitioners (ourselves included) in labelling bed properties. When we invert

for basal properties we are not solely inverting for ‘roughness’, ‘till friction angle’, or ‘friction’ at the ice-bed interface itself – we are likely inverting for all of these processes, and several more, simultaneously. We use ‘ideal circumstances’ here because the traction field is often one of the few tunable parameters in an ice-sheet model and so will in practice also account for so-called ‘compensating errors’ arising from incorrectly prescribed englacial temperature, ice viscosity, subglacial topography, and surface and basal mass balance (Berends and others, 2023). Last, while we use ‘glacier sliding’ throughout this paper to remain in keeping with its common usage, but make a distinction with ‘slip’ to refer strictly to ice-bed displacement; ‘glacier basal motion’ (e.g. Waller, 2001; Hubbard, 2002; Law and others, 2023) is probably a more precise term.

## 7 CONCLUSIONS

Glacier sliding is not a straightforward topic. Here, we have done our best to integrate existing understanding into a relatively straightforward framework. This is centred upon an inner flow (Fig. 5) comprised of potentially numerous sliding sub-processes (Fig. 4), which can be represented over a given region through Eq. 8. While it may be possible to reduce this complexity into a *relatively* simple aggregate equation (such as Eq. 20), we would advocate for the use of a power-law relationship, with careful selection of the  $m$  parameter based on the setting, due to its flexibility in representing both regularised-Coulomb and power-law end members.

Our coverage also highlights some clear priorities for future work. Principally, we still do not have a clear methodology for linking stick-slip sliding with continuous sliding relationships, and major questions remain regarding how best to incorporate  $N$  within sliding relationships, and how it may be expected to change at the decadal to centennial timescales relevant to projections of ice-sheet and glacier mass loss. The landscape factors influencing the balance of slip, deformation, and geometric resistance also remain unexplored in a quantitative manner, as does the importance and formation, or lack thereof, of subglacial cavitation at large scales. Overall, we hope that the framework presented here allows for a transparent approach to understanding glacier sliding, applying glacier sliding relationships to numerical models, and for directing future research.

## REFERENCES

- Abercrombie RE (2015) Investigating uncertainties in empirical Green’s function analysis of earthquake source parameters. *Journal of Geophysical Research: Solid Earth*, **120**(6), 4263–4277, ISSN 2169-9356 (doi: 10.1002/2015JB011984)
- Adams CJ, Iverson NR, Helanow C, Zoet LK and Bate CE (2021) Softening of Temperate Ice by Interstitial Water. *Frontiers in Earth Science*, **9**, 702761, ISSN 22966463 (doi: 10.3389/feart.2021.702761)
- Åkesson H, Morlighem M, O’Regan M and Jakobsson M (2021) Future Projections of Petermann Glacier Under Ocean Warming Depend Strongly on Friction Law. *Journal of Geophysical Research: Earth Surface*, **126**(6), e2020JF005921, ISSN 2169-9011 (doi: 10.1029/2020JF005921)
- Alley RB and Whillans IM (1984) Response of the East Antarctica ice sheet to sea-level rise. *Journal of Geophysical Research*, **89**(C4), 6487, ISSN 0148-0227 (doi: 10.1029/JC089iC04p06487)
- Arthern RJ and Gudmundsson GH (2010) Initialization of ice-sheet forecasts viewed as an inverse Robin problem. *Journal of Glaciology*, **56**(197), 527–533, ISSN 0022-1430 (doi: 10.3189/002214310792447699)
- Arya SPS (1973) Contribution of form drag on pressure ridges to the air stress on Arctic ice. *Journal of Geophysical Research*, **78**(30), 7092–7099, ISSN 2156-2202 (doi: 10.1029/JC078i030P07092)
- Aschwanden A, Fahnestock MA and Truffer M (2016) Complex Greenland outlet glacier flow captured. *Nature Communications*, **7**, 10524, ISSN 20411723 (doi: 10.1038/ncomms10524)
- Aschwanden A, Bartholomaeus TC, Brinkerhoff DJ and Truffer M (2021) Brief communication: A roadmap towards credible projections of ice sheet contribution to sea level. *Cryosphere*, **15**(12), 5705–5715, ISSN 19940424 (doi: 10.5194/TC-15-5705-2021)
- Ashmore DW and Bingham RG (2014) Antarctic subglacial hydrology: current knowledge and future challenges. *Antarctic Science*, **26**(06), 758–773, ISSN 0954-1020 (doi: 10.1017/S0954102014000546)
- Ashmore DW, Bingham RG, Ross N, Siegert MJ, Jordan TA and Mair DW (2020) Englacial Architecture and Age-Depth Constraints Across the West Antarctic Ice Sheet. *Geophysical Research Letters*, **47**(6), e2019GL086663, ISSN 1944-8007 (doi: 10.1029/2019GL086663)
- Atkins CB (2013) Geomorphological evidence of cold-based glacier activity in South Victoria Land, Antarctica. *Geological Society Special Publication*, **381**(1), 299–318, ISSN 03058719 (doi: https://doi.org/10.1144/SP381.18)
- Azzaro R, Bonforte A, D’Amico S, Guglielmino F and Scarfi L (2020) Stick-slip vs. stable sliding fault behaviour: A case-study using a multidisciplinary approach in the volcanic region of Mt. Etna (Italy). *Tectonophysics*, **790**, ISSN 00401951 (doi: 10.1016/j.tecto.2020.228554)

- Bahr DB and Rundle JB (1995) Theory of lattice Boltzmann simulations of glacier flow. *Journal of Glaciology*, **41**(139), 634–640, ISSN 0022-1430 (doi: 10.3189/S0022143000034948)
- Bahr DB and Rundle JB (1996) Stick-slip statistical mechanics at the bed of a glacier. *Geophysical Research Letters*, **23**(16), 2073–2076, ISSN 1944-8007 (doi: 10.1029/96GL02069)
- Baker RW (1981) Textural and Crystal-Fabric Anisotropies and the Flow of Ice Masses. *Science*, **211**(4486), 1043–1044, ISSN 00368075 (doi: 10.1126/SCIENCE.211.4486.1043)
- Balise MJ and Raymond CF (1985) Transfer of Basal Sliding Variations to the Surface of a Linearly Viscous Glacier. *Journal of Glaciology*, **31**(109), 308–318, ISSN 0022-1430 (doi: 10.3189/S002214300000664X)
- Barcheck CG, Schwartz SY and Tulaczyk S (2020) Icequake streaks linked to potential mega-scale glacial lineations beneath an Antarctic ice stream. *Geology*, **48**(2), 99–102, ISSN 0091-7613 (doi: 10.1130/G46626.1)
- Barnes P, Tabor D and Walker J (1971) The friction and creep of polycrystalline ice. *Proceedings of the Royal Society of London. A. Mathematical and Physical Sciences*, **324**(1557), 127–155, ISSN 0080-4630 (doi: 10.1098/RSPA.1971.0132)
- Bartholomew ID, Nienow P, Sole A, Mair D, Cowton T, King MA and Palmer S (2011) Seasonal variations in Greenland Ice Sheet motion: Inland extent and behaviour at higher elevations. *Earth and Planetary Science Letters*, **307**(3-4), 271–278, ISSN 0012821X (doi: 10.1016/j.epsl.2011.04.014)
- Batchelor GK (1967) *An Introduction to Fluid Dynamics*. Cambridge University Press, ISBN 9780521663960 (doi: 10.1017/CBO9780521663960)
- Beckmann J and Winkelmann R (2023) Effects of extreme melt events on ice flow and sea level rise of the Greenland Ice Sheet. *Cryosphere*, **17**(7), 3083–3099, ISSN 19940424 (doi: 10.5194/TC-17-3083-2023)
- Bell RE, Ferraccioli F, Creyts TT, Braaten D, Corr H, Das I, Damaske D, Frearson N, Jordan T, Rose K, Studinger M and Wolovick M (2011) Widespread Persistent Thickening of the East Antarctic Ice Sheet by Freezing from the Base. *Science*, **331**(6024), 1592–1595, ISSN 00368075 (doi: 10.1126/SCIENCE.1200109)
- Benn DI and Evans DJA (2010) *Glaciers and Glaciation*. Routledge, London, 2 edition
- Bercovici D (2003) The generation of plate tectonics from mantle convection. *Earth and Planetary Science Letters*, **205**(3-4), 107–121, ISSN 0012-821X (doi: 10.1016/S0012-821X(02)01009-9)
- Berends CJ, van de Wal RSW, van den Akker T and Lipscomb WH (2023) Compensating errors in inversions for subglacial bed roughness: same steady state, different dynamic response. *The Cryosphere*, **17**(4), 1585–1600, ISSN 1994-0424 (doi: 10.5194/TC-17-1585-2023)
- Biegel RL, Sammis CG and Dieterich JH (1989) The frictional properties of a simulated gouge having a fractal particle distribution. *Journal of Structural Geology*, **11**(7), 827–846, ISSN 0191-8141 (doi: 10.1016/0191-8141(89)90101-6)
- Bindschadler RA, King MA, Alley RB, Anandakrishnan S and Padman L (2003) Tidally controlled stick-slip discharge of a West Antarctic ice stream. *Science*, **301**(5636), 1087–1089, ISSN 00368075 (doi: https://doi.org/10.1126/science.1087231)
- Bingham RG and Siegert MJ (2009) Quantifying subglacial bed roughness in Antarctica: implications for ice-sheet dynamics and history. *Quaternary Science Reviews*, **28**(3-4), 223–236, ISSN 0277-3791 (doi: 10.1016/J.QUASCIREV.2008.10.014)
- Bingham RG, Vaughan DG, King EC, Davies D, Cornford SL, Smith AM, Arthern RJ, Brisbourne AM, De Rydt J, Graham AG, Spagnolo M, Marsh OJ and Shean DE (2017) Diverse landscapes beneath Pine Island Glacier influence ice flow. *Nature Communications*, **8**, 1618, ISSN 2041-1723 (doi: 10.1038/s41467-017-01597-y)
- Björnsson H, Pálsson F, Sigurdsson O and Flowers GE (2003) Surges of glaciers in Iceland. *Annals of Glaciology*, **36**, 82–90, ISSN 0260-3055 (doi: 10.3189/172756403781816365)
- Blake EW (1992) *The deforming bed beneath a surge-type glacier: measurement of mechanical and electrical properties*. Ph.D. thesis, The University of British Columbia, Vancouver (doi: 10.14288/1.0052926)
- Bons PD, Jansen D, Mundel F, Bauer CC, Binder T, Eisen O, Jessell MW, Llorens MG, Steinbach F, Steinhage D and Weikusat I (2016) Converging flow and anisotropy cause large-scale folding in Greenland's ice sheet. *Nature Communications*, **7**, 11427, ISSN 2041-1723 (doi: 10.1038/ncomms11427)
- Bons PD, Kleiner T, Llorens MG, Prior DJ, Sachau T, Weikusat I and Jansen D (2018) Greenland Ice Sheet: Higher Nonlinearity of Ice Flow Significantly Reduces Estimated Basal Motion. *Geophysical Research Letters*, **45**(13), 6542–6548, ISSN 00948276 (doi: 10.1029/2018GL078356)
- Booth AD, Clark RA, Kulesa B, Murray T, Carter J, Doyle S and Hubbard A (2012) Thin-layer effects in glaciological seismic amplitude-versus-angle (AVA) analysis: Implications for characterising a subglacial till unit, Russell Glacier, West Greenland. *Cryosphere*, **6**(4), 909–922, ISSN 19940416 (doi: 10.5194/TC-6-909-2012)
- Bougamont M, Christoffersen P, Hubbard AL, Fitzpatrick AA, Doyle SH and Carter SP (2014) Sensitive response of the Greenland Ice Sheet to surface melt drainage over a soft bed. *Nature Communications*, **5**, 5052, ISSN 20411723 (doi: 10.1038/ncomms6052)
- Boulton GS and Hindmarsh RC (1987) Sediment deformation beneath glaciers: Rheology and geological consequences. *Journal of Geophysical Research: Solid Earth*, **92**(B9), 9059–9082, ISSN 2156-2202 (doi: 10.1029/JB092IB09P09059)

- Bowling JS, Livingstone SJ, Sole AJ and Chu W (2019) Distribution and dynamics of Greenland subglacial lakes. *Nature Communications*, **10**(1), ISSN 20411723 (doi: 10.1038/s41467-019-10821-w)
- Bradley AT and Hewitt IJ (2024) Tipping point in ice-sheet grounding-zone melting due to ocean water intrusion. *Nature Geoscience* 2024 17:7, **17**(7), 631–637, ISSN 1752-0908 (doi: 10.1038/s41561-024-01465-7)
- Brondex J, Gillet-Chaulet F and Gagliardini O (2019) Sensitivity of centennial mass loss projections of the Amundsen basin to the friction law. *Cryosphere*, **13**, 177–195, ISSN 19940424 (doi: 10.5194/tc-13-177-2019)
- Budd WF and Jacka TH (1989) A review of ice rheology for ice sheet modelling. *Cold Regions Science and Technology*, **16**(2), 107–144, ISSN 0165232X (doi: 10.1016/0165-232X(89)90014-1)
- Budd WF, Keage PL and Blundy NA (1979) Empirical Studies of Ice Sliding. *Journal of Glaciology*, **23**(89), 157–170, ISSN 0022-1430 (doi: 10.3189/S0022143000029804)
- Budd WF, Jenssen D and Smith IN (1984) A Three-Dimensional Time-Dependent Model of the West Antarctic Ice Sheet. *Annals of Glaciology*, **5**, 29–36, ISSN 0260-3055 (doi: 10.3189/1984AOG5-1-29-36)
- Campin JM and Goosse H (1999) Parameterization of density-driven downsloping flow for a coarse-resolution ocean model in z-coordinate. *Tellus A: Dynamic Meteorology and Oceanography*, **51**(3), 412–430, ISSN 02806495 (doi: 10.3402/TELLUSA.V51I3.13468)
- Catania GA, Stearns LA, Sutherland DA, Fried MJ, Bartholomaeus TC, Morlighem M, Shroyer E and Nash J (2018) Geometric Controls on Tidewater Glacier Retreat in Central Western Greenland. *Journal of Geophysical Research: Earth Surface*, **123**(8), 2024–2038, ISSN 2169-9011 (doi: 10.1029/2017JF004499)
- Chandler DM, Hubbard AL, Hubbard BP and Nienow PW (2006) A Monte Carlo error analysis for basal sliding velocity calculations. *Journal of Geophysical Research*, **111**(F4), F04005, ISSN 0148-0227 (doi: 10.1029/2006JF000476)
- Chandler DM, Wadham JL, Lis GP, Cowton T, Sole A, Bartholomew I, Telling J, Nienow P, Bagshaw EB, Mair D, Vinen S and Hubbard A (2013) Evolution of the subglacial drainage system beneath the Greenland Ice Sheet revealed by tracers. *Nature Geoscience*, **6**(3), 195–198, ISSN 1752-0894 (doi: 10.1038/ngeo1737)
- Choi Y, Seroussi H, Gardner A and Schlegel NJ (2022) Uncovering Basal Friction in Northwest Greenland Using an Ice Flow Model and Observations of the Past Decade. *Journal of Geophysical Research: Earth Surface*, **127**(10), e2022JF006710, ISSN 2169-9011 (doi: 10.1029/2022JF006710)
- Chu VW (2014) Greenland ice sheet hydrology. *Progress in Physical Geography*, **38**(1), 19–54, ISSN 0309-1333 (doi: 10.1177/0309133313507075)
- Clark PU and Hansel AK (1989) Clast ploughing, lodgement and glacier sliding over a soft glacier bed. *Boreas*, **18**(3), 201–207, ISSN 1502-3885 (doi: 10.1111/J.1502-3885.1989.TB00392.X)
- Clarke GK (2005) Subglacial processes. *Annual Review of Earth and Planetary Sciences*, **33**(1), 247–276, ISSN 0084-6597 (doi: 10.1146/annurev.earth.33.092203.122621)
- Cohen D, Iverson NR, Hooyer TS, Fischer UH, Jackson M and Moore PL (2005) Debris-bed friction of hard-bedded glaciers. *Journal of Geophysical Research: Earth Surface*, **110**(F2), 2007, ISSN 2156-2202 (doi: 10.1029/2004JF000228)
- Cook AJ, Holland PR, Meredith MP, Murray T, Luckman A and Vaughan DG (2016) Ocean forcing of glacier retreat in the western Antarctic Peninsula. *Science*, **353**(6296), 283–286, ISSN 0036-8075 (doi: 10.1126/science.aae0017)
- Cook SJ, Knight PG, Waller RI, Robinson ZP and Adam WG (2007) The geography of basal ice and its relationship to glaciohydraulic supercooling: Svinafellsjökull, southeast Iceland. *Quaternary Science Reviews*, **26**(19–21), 2309–2315, ISSN 0277-3791 (doi: 10.1016/J.QUASCIREV.2007.07.010)
- Cook SJ, Swift DA, Graham DJ and Midgley NG (2011) Origin and significance of ‘dispersed facies’ basal ice: Svinafellsjökull, Iceland. *Journal of Glaciology*, **57**(204), 710–720, ISSN 0022-1430 (doi: 10.3189/002214311797409703)
- Coulomb C (1785) théorie des machines simples, en ayant égard de leurs parties et de la roideur des cordages. In *Mémoires de Mathématique et de Physique de l'Académie Royale des Sciences*, volume X, 131–332, Moutard, Paris, 1st edition
- Cuffey KM and Paterson WSB (2010) *The Physics of Glaciers*. Elsevier Science & Technology Books, Amsterdam, 4 edition, ISBN 9780080919126
- Cuffey KM, Conway H, Hallet B, Gades AM and Raymond CF (1999) Interfacial water in polar glaciers and glacier sliding at  $-17^{\circ}\text{C}$ . *Geophysical Research Letters*, **26**(6), 751–754, ISSN 1944-8007 (doi: 10.1029/1999GL900096)
- Damsgaard A, Egholm DL, Piotrowski JA, Tulaczyk S, Larsen NK and Tylmann K (2013) Discrete element modeling of subglacial sediment deformation. *Journal of Geophysical Research: Earth Surface*, **118**(4), 2230–2242, ISSN 2169-9011 (doi: 10.1002/2013JF002830)
- Damsgaard A, Cabrales-Vargas A, Suckale J and Goren L (2017) The Coupled Dynamics of Meltwater Percolation and Granular Deformation in the Sediment Layer Underlying Parts of the Big Ice Sheets. In *Proceedings of the 6th Biot Conference on Poromechanics*, 198–206, American Society of Civil Engineers, ISBN 9780784480779 (doi: 10.1061/9780784480779.024)
- Damsgaard A, Goren L and Suckale J (2020) Water pressure fluctuations control variability in sediment flux and slip dynamics beneath glaciers and ice streams. *Communications Earth &*

- Environment* 2020 1:1, 1(1), 1–8, ISSN 2662-4435 (doi: 10.1038/s43247-020-00074-7)
- Das SB, Joughin I, Behn MD, Howat IM, King MA, Lizarralde D and Bhatia MP (2008) Fracture propagation to the base of the Greenland Ice Sheet during supraglacial lake drainage. *Science (New York, N.Y.)*, **320**(5877), 778–81, ISSN 1095-9203 (doi: 10.1126/science.1153360)
- Davison BJ, Sole AJ, Livingstone SJ, Cowton TR and Nienow PW (2019) The influence of hydrology on the dynamics of land-terminating sectors of the Greenland ice sheet (doi: 10.3389/feart.2019.00010)
- Dawson EJ, Schroeder DM, Chu W, Mantelli E and Seroussi H (2024) Heterogeneous Basal Thermal Conditions Underpinning the Adélie-George V Coast, East Antarctica. *Geophysical Research Letters*, **51**(2), e2023GL105450, ISSN 1944-8007 (doi: 10.1029/2023GL105450)
- De Fleurian B, Werder MA, Beyer S, Brinkerhoff DJ, Delaney I, Dow CF, Downs J, Gagliardini O, Hoffman MJ, Hooke RL, Seguinot J and Sommers AN (2018) SHMIP The subglacial hydrology model intercomparison Project. *Journal of Glaciology*, **64**(248), 897–916, ISSN 0022-1430 (doi: 10.1017/JOG.2018.78)
- Dehecq A, Gourmelen N, Gardner AS, Brun F, Goldberg D, Nienow PW, Berthier E, Vincent C, Wagnon P and Trouvé E (2018) Twenty-first century glacier slowdown driven by mass loss in High Mountain Asia. *Nature Geoscience* 2018 12:1, **12**(1), 22–27, ISSN 1752-0908 (doi: 10.1038/s41561-018-0271-9)
- Desplanques Y (2014) Amontons-Coulomb friction laws, a review of the original manuscript. *SAE International Journal of Materials and Manufacturing*, **8**(1), 98–103, ISSN 19463987 (doi: 10.4271/2014-01-2489)
- Dieterich JH (1979) Modeling of rock friction: 1. Experimental results and constitutive equations. *Journal of Geophysical Research: Solid Earth*, **84**(B5), 2161–2168, ISSN 2156-2202 (doi: 10.1029/JB084IB05P02161)
- Dow CF, Hubbard A, Booth AD, Doyle SH, Gusmeroli A and Kulesa B (2013) Seismic evidence of mechanically weak sediments underlying Russell Glacier, West Greenland. *Annals of Glaciology*, **54**(64), 135–141, ISSN 02603055 (doi: 10.3189/2013AoG64A032)
- Dow CF, Kulesa B, Rutt IC, Tsai VC, Pimentel S, Doyle SH, van As D, Lindbäck K, Pettersson R, Jones GA and Hubbard A (2015) Modeling of subglacial hydrological development following rapid supraglacial lake drainage. *Journal of Geophysical Research: Earth Surface*, **120**(6), 1127–1147, ISSN 21699003 (doi: 10.1002/2014JF003333)
- Doyle SH, Hubbard A, Van De Wal RS, Box JE, Van As D, Scharrer K, Meierbachtol TW, Smeets PC, Harper JT, Johansson E, Mottram RH, Mikkelsen AB, Wilhelms F, Patton H, Christoffersen P and Hubbard B (2015) Amplified melt and flow of the Greenland ice sheet driven by late-summer cyclonic rainfall. *Nature Geoscience* 2014 8:8, **8**(8), 647–653, ISSN 1752-0908 (doi: 10.1038/ngeo2482)
- Doyle SH, Hubbard B, Christoffersen P, Young TJ, Hofstede C, Bougamont M, Box JE and Hubbard A (2018) Physical Conditions of Fast Glacier Flow: 1. Measurements From Boreholes Drilled to the Bed of Store Glacier, West Greenland. *Journal of Geophysical Research: Earth Surface*, **123**(2), 324–348, ISSN 21699003 (doi: 10.1002/2017JF004529)
- Doyle SH, Hubbard B, Christoffersen P, Law R, Hewitt DR, Neufeld JA, Schoonman CM, Chudley TR and Bougamont M (2021) Water flow through sediments and at the ice-sediment interface beneath Sermeq Kujalleq (Store Glacier), Greenland. *Journal of Glaciology*, 1–20, ISSN 0022-1430 (doi: 10.1017/JOG.2021.121)
- Duval P (1981) Creep and Fabrics of Polycrystalline Ice Under Shear and Compression. *Journal of Glaciology*, **27**(95), 129–140, ISSN 0022-1430 (doi: 10.3189/S002214300001128X)
- Echelmeyer K and Zhongxiang W (1987) Direct Observation of Basal Sliding and Deformation of Basal Drift at Sub-Freezing Temperatures. *Journal of Glaciology*, **33**(113), 83–98, ISSN 0022-1430 (doi: 10.3189/S0022143000005396)
- Ely JC, Stevens D, Clark CD and Butcher FE (2023) Numerical modelling of subglacial ribs, drumlins, herringbones, and mega-scale glacial lineations reveals their developmental trajectories and transitions. *Earth Surface Processes and Landforms*, **48**(5), 956–978, ISSN 1096-9837 (doi: 10.1002/ESP.5529)
- Engelhardt H and Kamb B (1997) Basal hydraulic system of a West Antarctic ice stream: constraints from borehole observations. *Journal of Glaciology*, **43**(144), 207–230, ISSN 0022-1430 (doi: 10.3189/S0022143000003166)
- Engelhardt H, Humphrey N, Kamb B and Fahnestock M (1990) Physical conditions at the base of a fast moving Antarctic ice stream. *Science*, **248**(4951), 57–59, ISSN 00368075 (doi: 10.1126/science.248.4951.57)
- Falcini FA, Rippin DM, Krabbendam M and Selby KA (2018) Quantifying bed roughness beneath contemporary and palaeo-ice streams. *Journal of Glaciology*, **64**(247), 822–834, ISSN 0022-1430 (doi: 10.1017/JOG.2018.71)
- Fetfatsidis KA, Gamache LM, Gorczyca JL, Sherwood JA, Jauffrès D and Chen J (2013) Design of an apparatus for measuring tool/fabric and fabric/fabric friction of woven-fabric composites during the thermostamping process. *International Journal of Material Forming*, **6**(1), 1–11, ISSN 19606214 (doi: 10.1007/S12289-011-1058-3/FIGURES/23)
- Fischer UH, Porter PR, Schuler T, Evans AJ and Gudmundsson GH (2001) Hydraulic and mechanical properties of glacial sediments beneath Unteraargletscher, Switzerland: implications for glacier basal motion. *Hydrological Processes*, **15**(18), 3525–3540, ISSN 1099-1085 (doi: 10.1002/HYP.349)

- Fitzsimons SJ, Mcmanus KJ and Lorrain RD (1999) Structure and strength of basal ice and substrate of a dry-based glacier: evidence for substrate deformation at sub-freezing temperatures. *Annals of Glaciology*, **28**, 236–240, ISSN 0260-3055 (doi: 10.3189/172756499781821878)
- Fowler A (1977) *Glacier Dynamics*. Ph.D. thesis, University of Oxford, Oxford
- Fowler AC (1981) A Theoretical Treatment of the Sliding of Glaciers in the Absence of Cavitation on JSTOR
- Fowler AC (1986) Sub-Temperate Basal Sliding. *Journal of Glaciology*, **32**(110), 3–5, ISSN 0022-1430 (doi: 10.3189/S0022143000006808)
- Fowler AC (2010) Weertman, Lliboutry and the development of sliding theory. *Journal of Glaciology*, **56**(200), 965–972, ISSN 0022-1430 (doi: 10.3189/002214311796406112)
- Fowler AC and Larson DA (1978) On the flow of polythermal glaciers - I. Model and preliminary analysis. *Proceedings of the Royal Society of London. A. Mathematical and Physical Sciences*, **363**(1713, Nov.1, 1978), 217–242, ISSN 0080-4630 (doi: 10.1098/RSPA.1978.0165)
- Fox RW, McDonald AT and Pritchard PJ (2006) *Introduction to fluid mechanics*. Wiley, 6 edition, ISBN 0471735582
- Frank T, Åkesson H, De Fleurian B, Morlighem M and Nisancioglu KH (2022) Geometric controls of tidewater glacier dynamics. *Cryosphere*, **16**(2), 581–601, ISSN 19940424 (doi: 10.5194/TC-16-581-2022)
- Franke S, Wolovick M, Drews R, Jansen D, Matsuoka K and Bons PD (2024) Sediment Freeze-On and Transport Near the Onset of a Fast-Flowing Glacier in East Antarctica. *Geophysical Research Letters*, **51**(6), e2023GL107164, ISSN 1944-8007 (doi: 10.1029/2023GL107164)
- Fretwell P, Pritchard HD, Vaughan DG, Bamber JL, Barrand NE, Bell R, Bianchi C, Bingham RG, Blankenship DD, Casassa G, Catania G, Callens D, Conway H and others (2013) Bedmap2: Improved ice bed, surface and thickness datasets for Antarctica. *Cryosphere*, **7**(1), 375–393, ISSN 19940416 (doi: 10.5194/tc-7-375-2013)
- Gagliardini O, Cohen D, Råback P and Zwinger T (2007) Finite-element modeling of subglacial cavities and related friction law. *Journal of Geophysical Research: Earth Surface*, **112**(F2), 2027, ISSN 2156-2202 (doi: 10.1029/2006JF000576)
- Garcia-Oteyza J, Oliva M, Palacios D, Fernández-Fernández JM, Schimmelpennig I, Andrés N, Antoniadis D, Christiansen HH, Humlum O, Léanni L, Jomelli V, Ruiz-Fernández J, Rinterknecht V, Lane TP, Adamson K, Aumaitre G, Bourlès D and Keddadouche K (2022) Late Glacial deglaciation of the Zackenberg area, NE Greenland. *Geomorphology*, **401**, 108125, ISSN 0169-555X (doi: 10.1016/J.GEOMORPH.2022.108125)
- Gilbert A, Gimbert F, Gagliardini O and Vincent C (2023) Inferring the Basal Friction Law From Long Term Changes of Glacier Length, Thickness and Velocity on an Alpine Glacier. *Geophysical Research Letters*, **50**(16), e2023GL104503, ISSN 1944-8007 (doi: 10.1029/2023GL104503)
- Gillet-Chaulet F, Gagliardini O, Meyssonier J, Montagnat M and Castelnau O (2005) A user-friendly anisotropic flow law for ice-sheet modeling. *Journal of Glaciology*, **51**(172), 3–14, ISSN 0022-1430 (doi: 10.3189/172756505781829584)
- Gillet-Chaulet F, Hindmarsh RCA, Corr HFJ, King EC and Jenkins A (2011) In-situ quantification of ice rheology and direct measurement of the Raymond Effect at Summit, Greenland using a phase-sensitive radar. *Geophysical Research Letters*, **38**(24), L24503, ISSN 1944-8007 (doi: 10.1029/2011GL049843)
- Gillet-Chaulet F, Gagliardini O, Seddik H, Nodet M, Durand G, Ritz C, Zwinger T, Greve R and Vaughan DG (2012) Greenland ice sheet contribution to sea-level rise from a new-generation ice-sheet model. *Cryosphere*, **6**(6), 1561–1576, ISSN 19940416 (doi: 10.5194/TC-6-1561-2012)
- Gillet-Chaulet F, Durand G, Gagliardini O, Mosbeux C, Mougint J, Rémy F and Ritz C (2016) Assimilation of surface velocities acquired between 1996 and 2010 to constrain the form of the basal friction law under Pine Island Glacier. *Geophysical Research Letters*, **43**(19), 311–10, ISSN 1944-8007 (doi: 10.1002/2016GL069937)
- Gimbert F, Gilbert A, Gagliardini O, Vincent C and Moreau L (2021) Do Existing Theories Explain Seasonal to Multi-Decadal Changes in Glacier Basal Sliding Speed? *Geophysical Research Letters*, **48**(15), e2021GL092858, ISSN 1944-8007 (doi: 10.1029/2021GL092858)
- Glen JW (1952) Experiments on the Deformation of Ice. *Journal of Glaciology*, **2**(12), 111–114, ISSN 0022-1430 (doi: 10.3189/s0022143000034067)
- Glen JW (1955) The creep of polycrystalline ice. *Proceedings of the Royal Society of London. Series A. Mathematical and Physical Sciences*, **228**(1175), 519–538 (doi: 10.1098/rspa.1955.0066)
- Goeller S, Steinhage D, Thoma M and Grosfeld K (2016) Assessing the subglacial lake coverage of Antarctica. *Annals of Glaciology*, **57**(72), 109–117, ISSN 0260-3055 (doi: 10.1017/AOG.2016.23)
- Goelzer H, Nowicki S, Payne A, Larour E, Seroussi H, Lipscomb WH, Gregory J, Abe-Ouchi A, Shepherd A, Simon E, Agosta C, Alexander P and Aschwanden A (2020) The future sea-level contribution of the Greenland ice sheet: A multi-model ensemble study of ISMIP6. *The Cryosphere*, **14**(9), 3071–3096, ISSN 19940424 (doi: 10.5194/TC-14-3071-2020)
- Goldsby DL and Kohlstedt DL (2001) Superplastic deformation of ice: Experimental observations. *Journal of Geophysical Research: Solid Earth*, **106**(B6), 11017–11030, ISSN 2169-9356 (doi: 10.1029/2000jb900336)

- Gomberg J, Beeler N and Blanpied M (2000) On rate-state and Coulomb failure models. *Journal of Geophysical Research: Solid Earth*, **105**(B4), 7857–7871, ISSN 2156-2202 (doi: 10.1029/1999JB900438)
- Goodsell B, Hambrey M and Glasser N (2005) Debris transport in a temperate valley glacier: Haut Glacier d’Arolla, Valais, Switzerland. *Journal of Glaciology*, **51**(172), 139–146, ISSN 0022-1430 (doi: 10.3189/172756505781829647)
- Gow AJ and Meese DA (1996) Nature of basal debris in the GISP2 and Byrd ice cores and its relevance to bed processes. *Annals of Glaciology*, **22**, 134–140, ISSN 0260-3055 (doi: 10.3189/1996AOG22-1-134-140)
- Gow AJ, Epstein S and Sheehy W (1979) On the Origin of Stratified Debris in Ice Cores from the Bottom of the Antarctic Ice Sheet. *Journal of Glaciology*, **23**(89), 185–192, ISSN 0022-1430 (doi: 10.3189/S0022143000029828)
- Grab M, Mattea E, Bauder A, Huss M, Rabenstein L, Hodel E, Linsbauer A, Langhammer L, Schmid L, Church G, Hellmann S, Deleze K, Schaer P, Lathion P, Farinotti D and Maurer H (2021) Ice thickness distribution of all Swiss glaciers based on extended ground-penetrating radar data and glaciological modeling. *Journal of Glaciology*, **67**(266), 1074–1092, ISSN 0022-1430 (doi: 10.1017/JOG.2021.55)
- Grocott J and McCaffrey KJ (2017) Basin evolution and destruction in an Early Proterozoic continental margin: the Rinkian fold–thrust belt of central West Greenland. *Journal of the Geological Society*, **174**(3), 453–467, ISSN 0016-7649 (doi: 10.1144/JGS2016-109)
- Gudmundsson GH (2011) Ice-stream response to ocean tides and the form of the basal sliding law. *Cryosphere*, **5**(1), 259–270, ISSN 19940416 (doi: 10.5194/TC-5-259-2011)
- Habermann M, Truffer M and Maxwell D (2013) Changing basal conditions during the speed-up of Jakobshavn Isbræ, Greenland. *Cryosphere*, **7**(6), 1679–1692, ISSN 19940424 (doi: 10.5194/TC-7-1679-2013)
- Hallet B, Lorrain R and Souchez R (1978) The composition of basal ice from a glacier sliding over limestones. *GSA Bulletin*, **89**(2), 314–320
- Hallet B, Gregory C, Stubbs C and Anderson R (1986) Measurements of ice motion over bedrock at subfreezing temperatures. In *Itteilungen der Versuchsanstalt für Wasser-bau, Hydrologie und Glaziologi an der ETH, Zurich*, 53–54, Zurich
- Hansen DD, Warburton KL, Zoet LK, Meyer CR, Rempel AW and Stubblefield AG (2024) Presence of Frozen Fringe Impacts Soft-Bedded Slip Relationship. *Geophysical Research Letters*, **51**(12), e2023GL107681, ISSN 1944-8007 (doi: 10.1029/2023GL107681)
- Harper JT, Humphrey NF, Meierbachtol TW, Graly JA and Fischer UH (2017) Borehole measurements indicate hard bed conditions, Kangerlussuaq sector, western Greenland Ice Sheet. *Journal of Geophysical Research: Earth Surface*, **122**(9), 1605–1618, ISSN 21699003 (doi: 10.1002/2017JF004201)
- Hart JK, Young DS, Baurley NR, Robson BA and Martinez K (2022) The seasonal evolution of subglacial drainage pathways beneath a soft-bedded glacier. *Communications Earth & Environment* **2022** 3:1, 3(1), 1–13, ISSN 2662-4435 (doi: 10.1038/s43247-022-00484-9)
- Hedfors J, Peyaud V, Pohjola VA, Jansson P and Petterson R (2003) Investigating the ratio of basal drag and driving stress in relation to bedrock topography during a melt season on Storglaciären, Sweden, using force-budget analysis. *Annals of Glaciology*, **37**, 263–268, ISSN 0260-3055 (doi: 10.3189/172756403781815861)
- Helanow C, Iverson NR, Zoet LK and Gagliardini O (2019) Sliding Relations for Glacier Slip With Cavities Over Three-Dimensional Beds. *Geophysical Research Letters*, **47**(3), e2019GL084924, ISSN 0094-8276 (doi: 10.1029/2019GL084924)
- Helanow C, Iverson NR, Woodard JB and Zoet LK (2021) A slip law for hard-bedded glaciers derived from observed bed topography. *Science Advances*, **7**(20), 7798–7812, ISSN 23752548 (doi: <https://doi.org/10.1126/sciadv.abe7798>)
- Helmstetter A, Nicolas B, Comon P and Gay M (2015) Basal icequakes recorded beneath an alpine glacier (Glacier d’Argentière, Mont Blanc, France): Evidence for stick-slip motion? *Journal of Geophysical Research: Earth Surface*, **120**(3), ISSN 21699011 (doi: 10.1002/2014JF003288)
- Hewitt DR, Chini GP and Neufeld JA (2018) The influence of a poroelastic till on rapid subglacial flooding and cavity formation. *Journal of Fluid Mechanics*, **855**, 1170–1207, ISSN 0022-1120 (doi: 10.1017/JFM.2018.624)
- Hoffman AO, Christianson K, Holschuh N, Case E, Kingslake J and Arthern R (2022) The Impact of Basal Roughness on Inland Thwaites Glacier Sliding. *Geophysical Research Letters*, **49**(14), e2021GL096564, ISSN 1944-8007 (doi: 10.1029/2021GL096564)
- Hoffman MJ, Andrews LC, Price SA, Catania GA, Neumann TA, Lüthi MP, Gulley J, Ryser C, Hawley RL and Morriss B (2016) Greenland subglacial drainage evolution regulated by weakly connected regions of the bed. *Nature Communications*, **7**, ISSN 20411723 (doi: 10.1038/ncomms13903)
- Hogan KA, Larter RD, Graham AG, Arthern R, Kirkham JD, Rebecca L T, Jordan TA, Clark R, Fitzgerald V, Wählin AK, Anderson JB, Hillenbrand CD, Nitsche FO, Simkins L, Smith JA, Gohl K, Erik Arndt J, Hong J and Wellner J (2020) Revealing the former bed of Thwaites Glacier using sea-floor bathymetry: Implications for warm-water routing and bed controls on ice flow and buttressing. *Cryosphere*, **14**(9), 2883–2908, ISSN 19940424 (doi: 10.5194/TC-14-2883-2020)

- Holschuh N, Christianson K, Paden J, Alley RB and Anandakrishnan S (2020) Linking postglacial landscapes to glacier dynamics using swath radar at Thwaites Glacier, Antarctica. *Geology*, **48**(3), 268–272, ISSN 0091-7613 (doi: 10.1130/G46772.1)
- Hooke R (1989) Englacial and Subglacial Hydrology: A Qualitative Review. *Arctic and Alpine Research*, **21**(3), 221–233 (doi: 10.1080/00040851.1989.12002734)
- Hooke RL, Hanson B, Iverson NR, Jansson P and Fischer UH (1997) Rheology of till beneath Storglaciären, Sweden. *Journal of Glaciology*, **43**(143), 172–179, ISSN 0022-1430 (doi: 10.3189/S0022143000002938)
- Hubbard B (2002) Direct measurement of basal motion at a hard-bedded, temperate glacier: Glacier de Tsanfleuron, Switzerland. *Journal of Glaciology*, **48**(160), 1–8, ISSN 0022-1430 (doi: 10.3189/172756502781831610)
- Hubbard B and Nienow P (1997) Alpine subglacial hydrology. *Quaternary Science Reviews*, **16**(9), 939–955, ISSN 0277-3791 (doi: 10.1016/S0277-3791(97)00031-0)
- Hubbard B and Sharp M (1989) Basal ice formation and deformation: A review (doi: 10.1177/030913338901300403)
- Hubbard B and Sharp M (1993) Weertman regelation, multiple refreezing events and the isotopic evolution of the basal ice layer. *Journal of Glaciology*, **39**(132), 275–291, ISSN 0022-1430 (doi: 10.3189/S002214300001594X)
- Hubbard B and Sharp M (1995) Basal ice facies and their formation in the Western Alps. *Arctic & Alpine Research*, **27**(4), 301–310, ISSN 00040851 (doi: 10.2307/1552023)
- Hubbard B, Cook S and Coulson H (2009) Basal ice facies: a review and unifying approach. *Quaternary Science Reviews*, **28**(19–20), 1956–1969, ISSN 02773791 (doi: 10.1016/j.quascirev.2009.03.005)
- Humphrey N, Kamb B, Fahnestock B and Engelhardt H (1993) Characteristics of the bed of the Lower Columbia Glacier, Alaska. *Journal of Geophysical Research: Solid Earth*, **98**(B1), 837–846, ISSN 2156-2202 (doi: 10.1029/92JB01869)
- Iken A (1981) The effect of the subglacial water pressure on the sliding velocity of a glacier in an idealized numerical model. *Journal of Glaciology*, **27**(97), 407–421
- Irvine-Fynn TD, Hodson AJ, Moorman BJ, Vatne G and Hubbard AL (2011) Polythermal glacier hydrology: A review (doi: 10.1029/2010RG000350)
- Iverson NR (1999) Coupling between a glacier and a soft bed: II Model results. *Journal of Glaciology*, **45**(149), 41–53, ISSN 0022-1430 (doi: 10.3189/S0022143000003026)
- Iverson NR (2000) Sediment entrainment by a soft-bedded glacier: a model based on regelation into the bed. *Earth Surface Processes and Landforms*, **25**(8), 881–893 (doi: 10.1002/1096-9837)
- Iverson NR (2010) Shear resistance and continuity of subglacial till: hydrology rules. *Journal of Glaciology*, **56**(200), 1104–1114, ISSN 0022-1430 (doi: 10.3189/002214311796406220)
- Iverson NR and Iverson RM (2001) Distributed shear of subglacial till due to Coulomb slip. *Journal of Glaciology*, **47**(158), 481–488, ISSN 0022-1430 (doi: 10.3189/172756501781832115)
- Iverson NR, Jansson P and Hooke RL (1994) In-situ measurement of the strength of deforming subglacial till. *Journal of Glaciology*, **40**(136), 497–503, ISSN 0022-1430 (doi: 10.3189/S0022143000012375)
- Iverson NR, Hanson B, Hooke RLB and Jansson P (1995) Flow Mechanism of Glaciers on Soft Beds. *Science*, **267**(5194), 80–81, ISSN 00368075 (doi: 10.1126/SCIENCE.267.5194.80)
- Iverson NR, Baker RW and Hooyer TS (1997) A ring-shear device for the study of till deformation: Tests on tills with contrasting clay contents. *Quaternary Science Reviews*, **16**(9), 1057–1066, ISSN 0277-3791 (doi: 10.1016/S0277-3791(97)00036-X)
- Iverson NR, Hooyer TS and Baker RW (1998) Ring-shear studies of till deformation: Coulomb-plastic behavior and distributed strain in glacier beds. *Journal of Glaciology*, **44**(148), 634–642, ISSN 0022-1430 (doi: 10.3189/S0022143000002136)
- Iverson NR, Cohen D, Hooyer TS, Fischer UH, Jackson H, Moore PL, Lappégard G and Kohler J (2003) Effects of basal debris on glacier flow. *Science*, **301**(5629), 81–84, ISSN 00368075 (doi: https://doi.org/10.1126/science.1083086)
- Jagannathan A, Srinivasan K, McWilliams JC, Molemaker J and Stewart AL (2023) Evolution of Bottom Boundary Layers on Three Dimensional Topography—Buoyancy Adjustment and Instabilities. *Journal of Geophysical Research: Oceans*, **128**(4), e2023JC019705, ISSN 2169-9291 (doi: 10.1029/2023JC019705)
- Jager E, Gillet-Chaulet F, Mouginot J and Millan R (2024) Validating ensemble historical simulations of Upernavik Isström (1985–2019) using observations of surface velocity and elevation. *Journal of Glaciology*, **70**, e36, ISSN 0022-1430 (doi: 10.1017/JOG.2024.10)
- Jenssen D (1977) A Three-Dimensional Polar Ice-Sheet Model. *Journal of Glaciology*, **18**(80), 373–389, ISSN 0022-1430 (doi: 10.3189/S0022143000021067)
- Jordan TA, Thompson S, Kulassa B and Ferraccioli F (2023) Geological sketch map and implications for ice flow of Thwaites Glacier, West Antarctica, from integrated aerogeophysical observations. *Science Advances*, **9**(22), ISSN 23752548 (doi: https://doi.org/10.1126/sciadv.adf2639)
- Joughin I, Tulaczyk S, Bamber JL, Blankenship D, Holt JW, Scambos T and Vaughan DG (2009) Basal conditions for Pine Island and Thwaites Glaciers, West Antarctica, determined using satellite and airborne data. *Journal of Glaciology*, **55**(190), 245–257, ISSN 0022-1430 (doi: 10.3189/002214309788608705)

- Joughin I, Smith BE and Holland DM (2010) Sensitivity of 21st century sea level to ocean-induced thinning of Pine Island Glacier, Antarctica. *Geophysical Research Letters*, **37**(20), ISSN 1944-8007 (doi: 10.1029/2010GL044819)
- Joughin I, Smith BE and Schoof CG (2019) Regularized Coulomb Friction Laws for Ice Sheet Sliding: Application to Pine Island Glacier, Antarctica. *Geophysical Research Letters*, **46**(9), 4764–4771, ISSN 0094-8276 (doi: 10.1029/2019GL082526)
- Jouvet G and Huss M (2019) Future retreat of Great Aletsch Glacier. *Journal of Glaciology*, **65**(253), 869–872, ISSN 0022-1430 (doi: 10.1017/JOG.2019.52)
- Jungdal-Olesen G, Andersen JL, Born A and Pedersen VK (2024) The influence of glacial landscape evolution on Scandinavian ice-sheet dynamics and dimensions. *Cryosphere*, **18**(4), 1517–1532, ISSN 19940424 (doi: 10.5194/TC-18-1517-2024)
- Kamb B (1970) Sliding motion of glaciers: Theory and observation. *Reviews of Geophysics*, **8**(4), 673–728, ISSN 1944-9208 (doi: 10.1029/RG008I004P00673)
- Kamb B (1987) Glacier surge mechanism based on linked cavity configuration of the basal water conduit system. *Journal of Geophysical Research*, ISSN 0148-0227 (doi: 10.1029/JB092iB09p09083)
- Kamb B (1991) Rheological nonlinearity and flow instability in the deforming bed mechanism of ice stream motion. *Journal of Geophysical Research: Solid Earth*, **96**(B10), 16585–16595, ISSN 2156-2202 (doi: 10.1029/91JB00946)
- Kamb B and Lachapelle E (1964) Direct Observation of the Mechanism of Glacier Sliding Over Bedrock\*. *Journal of Glaciology*, **5**(38), 159–172, ISSN 0022-1430 (doi: 10.3189/S0022143000028756)
- Katz RF and Worster MG (2010) Stability of ice-sheet grounding lines. *Proceedings of the Royal Society A: Mathematical, Physical and Engineering Sciences*, **466**(2118), 1597–1620, ISSN 14712946 (doi: 10.1098/RSPA.2009.0434)
- Khan SA, Choi Y, Morlighem M, Rignot E, Helm V, Humbert A, Mouginot J, Millan R, Kjær KH and Bjørk AA (2022) Extensive inland thinning and speed-up of Northeast Greenland Ice Stream. *Nature* 2022 611:7937, **611**(7937), 727–732, ISSN 1476-4687 (doi: 10.1038/s41586-022-05301-z)
- Klint KES, Engström J, Parmenter A, Ruskeeniemi T, Liljedahl LC and Lehtinen A (2013) Lineament mapping and geological history of the Kangerlussuaq region, southern West Greenland. *GEUS Bulletin*, **28**(28), 57–60, ISSN 2597-2154 (doi: 10.34194/GEUSB.V28.4725)
- Knight PG (1997) The basal ice layer of glaciers and ice sheets. *Quaternary Science Reviews*, **16**(9), 975–993, ISSN 0277-3791 (doi: 10.1016/S0277-3791(97)00033-4)
- Knight PG, Waller RI, Patterson CJ, Jones AP and Robinson ZP (2002) Discharge of debris from ice at the margin of the Greenland ice sheet. *Journal of Glaciology*, **48**(161), 192–198, ISSN 0022-1430 (doi: 10.3189/172756502781831359)
- Koellner S, Parizek BR, Alley RB, Muto A and Holschuh N (2019) The impact of spatially-variable basal properties on outlet glacier flow. *Earth and Planetary Science Letters*, **515**, 200–208, ISSN 0012-821X (doi: 10.1016/J.EPSL.2019.03.026)
- Köpfl M, Gräff D, Lipovsky BP, Selvadurai PA, Farinotti D and Walter F (2022) Hydraulic Conditions for Stick-Slip Tremor Beneath an Alpine Glacier. *Geophysical Research Letters*, **49**(21), ISSN 19448007 (doi: 10.1029/2022GL100286)
- Krabbendam M (2016) Sliding of temperate basal ice on a rough, hard bed: creep mechanisms, pressure melting, and implications for ice streaming. *The Cryosphere*, **10**(5), 1915–1932, ISSN 1994-0424 (doi: 10.5194/tc-10-1915-2016)
- Krim J (1996) Friction at the Atomic Scale. *Scientific American*, 74–80
- Kufner SK, Brisbourne AM, Smith AM, Hudson TS, Murray T, Schlegel R, Kendall JM, Anandakrishnan S and Lee I (2021) Not all Icequakes are Created Equal: Basal Icequakes Suggest Diverse Bed Deformation Mechanisms at Rutford Ice Stream, West Antarctica. *Journal of Geophysical Research: Earth Surface*, **126**(3), ISSN 21699011 (doi: 10.1029/2020JF006001)
- Kulesa B, Hubbard AL, Booth AD, Bougamont M, Dow CF, Doyle SH, Christoffersen P, Lindbäck K, Pettersson R, Fitzpatrick AA and Jones GA (2017) Seismic evidence for complex sedimentary control of Greenland Ice Sheet flow. *Science Advances*, **3**(8), e1603071, ISSN 23752548 (doi: https://doi.org/10.1126/sciadv.1603071)
- Kyrke-Smith TM, Gudmundsson GH and Farrell PE (2018) Relevance of detail in basal topography for basal slipperiness inversions: A case study on Pine Island Glacier, Antarctica. *Frontiers in Earth Science*, **11**, 33, ISSN 22966463 (doi: https://doi.org/10.3389/feart.2018.00033)
- Larour E, Seroussi H, Morlighem M and Rignot E (2012) Continental scale, high order, high spatial resolution, ice sheet modeling using the Ice Sheet System Model (ISSM). *Journal of Geophysical Research: Earth Surface*, **117**(F1), 1022, ISSN 2156-2202 (doi: 10.1029/2011JF002140)
- Law R, Christoffersen P, Hubbard B, Doyle SH, Chudley TR, Schoonman C, Bougamont M, des Tombe B, Schilperoort B, Kechavarzi C, Booth A and Young TJ (2021) Thermodynamics of a fast-moving Greenlandic outlet glacier revealed by fiber-optic distributed temperature sensing. *Science Advances*, **7**(20), eabe7136 (doi: https://doi.org/10.1126/sciadv.abe7136)

- Law R, Christoffersen P, Mackie E, Cook S, Haseloff M and Gagliardini O (2023) Complex motion of Greenland Ice Sheet outlet glaciers with basal temperate ice (doi: 10.1126/SCIADV.ABQ5180)
- Lawson DE and Kulla JB (1978) An Oxygen Isotope Investigation of the Origin of the Basal Zone of the Matanuska Glacier, Alaska. *https://doi.org/10.1086/649736*, **86**(6), 673–685, ISSN 0022-1376 (doi: 10.1086/649736)
- Leitchenkov GL, Antonov AV, Luneov PI and Lipenkov VY (2016) Geology and environments of subglacial Lake Vostok. *Philosophical Transactions of the Royal Society A: Mathematical, Physical and Engineering Sciences*, **374**(2059), ISSN 1364503X (doi: 10.1098/RSTA.2014.0302)
- Lile RC (1978) The Effect of Anisotropy on the Creep of Polycrystalline Ice. *Journal of Glaciology*, **21**(85), 475–483, ISSN 0022-1430 (doi: 10.3189/S0022143000033621)
- Lippert EYH, Morlighem M, Cheng G and Khan SA (2024) Modeling a Century of Change: Kangerlussuaq Glacier's Mass Loss From 1933 to 2021. *Geophysical Research Letters*, **51**(4), e2023GL106286, ISSN 1944-8007 (doi: 10.1029/2023GL106286)
- Liu E, Liu EW, Räss L, Herman F, Podladchikov Y and Suckale J (2023) Spontaneous Formation of an Internal Shear Band in Ice Flowing over Topographically Variable Bedrocks 2 (doi: 10.22541/essoar.167898501.11505896/v1)
- Lliboutry L (1966) Bottom temperatures and basal low-velocity layer in an ice sheet. *Journal of Geophysical Research*, **71**(10), 2535–2543, ISSN 2156-2202 (doi: 10.1029/JZ071I010P02535)
- Lliboutry L (1968) General Theory of Subglacial Cavitation and Sliding of Temperate Glaciers. *Journal of Glaciology*, **7**(49), 21–58, ISSN 0022-1430 (doi: 10.3189/S0022143000020396)
- Lliboutry L (1971) Permeability, Brine Content and Temperature of Temperate Ice. *Journal of Glaciology*, **10**(58), 15–29, ISSN 0022-1430 (doi: 10.3189/S002214300001296x)
- Lliboutry L (1979) Local Friction Laws for Glaciers: A Critical Review and New Openings. *Journal of Glaciology*, **23**(89), 67–95
- MacAyeal DR (2019) Revisiting Weertman's tombstone bed. *Annals of Glaciology*, **60**(80), 21–29, ISSN 0260-3055 (doi: 10.1017/AOG.2019.31)
- MacCready P, Pawlak G and Edwards K (2003) Form drag on ocean flows. In *Near boundary processes and their parameterization: Proc. 13th'Aha Huliko'a Hawaiian Winter Workshop*
- Macgregor JA, Fahnestock MA, Catania GA, Paden JD, Prasad Gogineni S, Young SK, Rybarski SC, Mabrey AN, Wagman BM and Morlighem M (2015) Radiostratigraphy and age structure of the Greenland Ice Sheet. *Journal of Geophysical Research: Earth Surface*, **120**(2), 212–241, ISSN 21699011 (doi: 10.1002/2014JF003215)
- MacGregor JA, Fahnestock MA, Catania GA, Aschwanden A, Clow GD, Colgan WT, Gogineni SP, Morlighem M, Nowicki SMJ, Paden JD, Price SF and Seroussi H (2016) A synthesis of the basal thermal state of the Greenland Ice Sheet. *Journal of Geophysical Research: Earth Surface*, **121**(7), 1328–1350, ISSN 21699003 (doi: 10.1002/2015JF003803)
- MacKie EJ, Schroeder DM, Zuo C, Yin Z and Caers J (2021) Stochastic modeling of subglacial topography exposes uncertainty in water routing at Jakobshavn Glacier. *Journal of Glaciology*, **67**(261), 75–83, ISSN 00221430 (doi: 10.1017/jog.2020.84)
- Maier N, Humphrey N, Harper J and Meierbachtol T (2019) Sliding dominates slow-flowing margin regions, Greenland Ice Sheet. *Science Advances*, **5**(7), eaaw5406, ISSN 23752548 (doi: 10.1126/sciadv.aaw5406)
- Maier N, Gimbert F, Gillet-Chaulet F and Gilbert A (2021) Basal traction mainly dictated by hard-bed physics over grounded regions of Greenland. *Cryosphere*, **15**(3), 1435–1451, ISSN 19940424 (doi: 10.5194/tc-15-1435-2021)
- Maier N, Gimbert F and Gillet-Chaulet F (2022) Threshold response to melt drives large-scale bed weakening in Greenland. *Nature* **2022** 607:7920, **607**(7920), 714–720, ISSN 1476-4687 (doi: 10.1038/s41586-022-04927-3)
- Mangerud J, Hughes AL, Sæle TH and Svendsen JI (2019) Ice-flow patterns and precise timing of ice sheet retreat across a dissected fjord landscape in western Norway. *Quaternary Science Reviews*, **214**, ISSN 02773791 (doi: 10.1016/j.quascirev.2019.04.032)
- Mantelli E, Haseloff M and Schoof C (2019) Ice sheet flow with thermally activated sliding. Part 1: the role of advection. *Proceedings of the Royal Society A*, **475**(2230), ISSN 14712946 (doi: 10.1098/RSPA.2019.0410)
- Martín C, Navarro F, Otero J, Cuadrado ML and Corcuera MI (2004) Three-dimensional modelling of the dynamics of Johnsons Glacier, Livingston Island, Antarctica. *Annals of Glaciology*, **39**, 1–8, ISSN 0260-3055 (doi: 10.3189/172756404781814537)
- McCarthy C, Savage H and Nettles M (2017) Temperature dependence of ice-on-rock friction at realistic glacier conditions. *Philosophical Transactions of the Royal Society A: Mathematical, Physical and Engineering Sciences*, **375**(2086), ISSN 1364503X (doi: 10.1098/RSTA.2015.0348)
- Meyer CR, Downey AS and Rempel AW (2018) Freeze-on limits bed strength beneath sliding glaciers. *Nature Communications*, **9**(1), 1–6, ISSN 20411723 (doi: 10.1038/s41467-018-05716-1)
- Millstein JD, Minchew BM and Pegler SS (2022) Ice viscosity is more sensitive to stress than commonly assumed. *Communications Earth & Environment* **2022** 3:1, **3**(1), 1–7, ISSN 2662-4435 (doi: 10.1038/s43247-022-00385-x)

- Minchow B and Joughin I (2020a) Toward a universal glacier slip law. *Science*, **368**(6486), 29–30, ISSN 10959203 (doi: <https://doi.org/10.1126/science.abb3566>)
- Minchow B and Joughin I (2020b) Toward a universal glacier slip law: A new friction rule may describe ice flow over rigid or deformable surfaces. *Science*, **368**(6486), 29–30, ISSN 10959203 (doi: [10.1126/SCIENCE.ABB3566/ASSET/94F6D0C2-85DC-4578-B986-EAC2235A4C96/ASSETS/GRAPHIC/368%29%29F2.JPG](https://doi.org/10.1126/SCIENCE.ABB3566/ASSET/94F6D0C2-85DC-4578-B986-EAC2235A4C96/ASSETS/GRAPHIC/368%29%29F2.JPG))
- Minchow B, Simons M, Björnsson H, Pálsson F, Morlighem M, Seroussi H, Larour E and Hensley S (2016) Plastic bed beneath Hofsjökull Ice Cap, central Iceland, and the sensitivity of ice flow to surface meltwater flux. *Journal of Glaciology*, **62**(231), 147–158, ISSN 0022-1430 (doi: [10.1017/JOG.2016.26](https://doi.org/10.1017/JOG.2016.26))
- Minchow BM, Meyer CR, Pegler SS, Lipovsky BP, Rempel AW, Hilmar Gudmundsson G and Iverson NR (2019) Comment on “Friction at the bed does not control fast glacier flow” (doi: [10.1126/science.aau6055](https://doi.org/10.1126/science.aau6055))
- Moon T, Joughin I, Smith B, van den Broeke MR, van de Berg WJ, Noël B and Usher M (2014) Distinct patterns of seasonal Greenland glacier velocity. *Geophysical Research Letters*, **41**(20), 7209–7216, ISSN 00948276 (doi: [10.1002/2014GL061836](https://doi.org/10.1002/2014GL061836))
- Morlighem M, Rignot E, Seroussi H, Larour E, Ben Dhia H and Aubry D (2010) Spatial patterns of basal drag inferred using control methods from a full-Stokes and simpler models for Pine Island Glacier, West Antarctica. *Geophysical Research Letters*, **37**(14), ISSN 1944-8007 (doi: [10.1029/2010GL043853](https://doi.org/10.1029/2010GL043853))
- Morlighem M, Seroussi H, Larour E and Rignot E (2013) Inversion of basal friction in Antarctica using exact and incomplete adjoints of a higher-order model. *Journal of Geophysical Research: Earth Surface*, **118**(3), ISSN 21699011 (doi: [10.1002/jgrf.20125](https://doi.org/10.1002/jgrf.20125))
- Morlighem M, Williams CN, Rignot E, An L, Arndt JE, Bamber JL, Catania G, Chauché N, Dowdeswell JA, Dorschel B, Fenty I, Hogan K, Howat I and others (2017) BedMachine v3: Complete Bed Topography and Ocean Bathymetry Mapping of Greenland From Multibeam Echo Sounding Combined With Mass Conservation. *Geophysical Research Letters*, **44**(21), 11051–11061, ISSN 19448007 (doi: [10.1002/2017GL074954](https://doi.org/10.1002/2017GL074954))
- Munevar Garcia S, Miller LE, Falcini FAM and Stearns LA (2023) Characterizing bed roughness on the Antarctic continental margin. *Journal of Glaciology*, 1–12, ISSN 0022-1430 (doi: [10.1017/JOG.2023.88](https://doi.org/10.1017/JOG.2023.88))
- Murray T and Porter PR (2001) Basal conditions beneath a soft-bedded polythermal surge-type glacier: Bakaninbreen, Svalbard. *Quaternary International*, **86**(1), 103–116, ISSN 1040-6182 (doi: [10.1016/S1040-6182\(01\)00053-2](https://doi.org/10.1016/S1040-6182(01)00053-2))
- Nakakuki T and Mura E (2013) Dynamics of slab rollback and induced back-arc basin formation. *Earth and Planetary Science Letters*, **361**, 287–297, ISSN 0012-821X (doi: [10.1016/J.EPSL.2012.10.031](https://doi.org/10.1016/J.EPSL.2012.10.031))
- Neave KG and Savage JC (1970) Icequakes on the Athabasca Glacier. *J Geophys Res*, **75**(8)
- Nienow PW, Sole AJ, Slater DA and Cowton TR (2017) Recent Advances in Our Understanding of the Role of Meltwater in the Greenland Ice Sheet System. *Current Climate Change Reports*, **3**(4), 330–344, ISSN 2198-6061 (doi: [10.1007/s40641-017-0083-9](https://doi.org/10.1007/s40641-017-0083-9))
- Nye JF (1952) The Mechanics of Glacier Flow. *Journal of Glaciology*, **2**(12), 82–93, ISSN 0022-1430 (doi: [10.3189/S0022143000033967](https://doi.org/10.3189/S0022143000033967))
- Nye JF (1969) A calculation on the sliding of ice over a wavy surface using a Newtonian viscous approximation. *Proceedings of the Royal Society of London. A. Mathematical and Physical Sciences*, **311**(1506), 445–467, ISSN 0080-4630 (doi: [10.1098/RSPA.1969.0127](https://doi.org/10.1098/RSPA.1969.0127))
- Nye JF (1970) Glacier sliding without cavitation in a linear viscous approximation. *Proceedings of the Royal Society of London. A. Mathematical and Physical Sciences*, **315**(1522), 381–403, ISSN 0080-4630 (doi: [10.1098/RSPA.1970.0050](https://doi.org/10.1098/RSPA.1970.0050))
- Oswald GK and Gogineni SP (2012) Mapping basal melt under the northern Greenland ice sheet. *IEEE Transactions on Geoscience and Remote Sensing*, **50**(2), 585–592, ISSN 01962892 (doi: [10.1109/TGRS.2011.2162072](https://doi.org/10.1109/TGRS.2011.2162072))
- Parizek BR, Christianson K, Anandakrishnan S, Alley RB, Walker RT, Edwards RA, Wolfe DS, Bertini GT, Rinehart SK, Bind-schadler RA and Nowicki SM (2013) Dynamic (in)stability of Thwaites Glacier, West Antarctica. *Journal of Geophysical Research: Earth Surface*, **118**(2), 638–655, ISSN 2169-9011 (doi: [10.1002/JGRF.20044](https://doi.org/10.1002/JGRF.20044))
- Paterson WS (1991) Why ice-age ice is sometimes “soft”. *Cold Regions Science and Technology*, **20**(1), 75–98, ISSN 0165-232X (doi: [10.1016/0165-232X\(91\)90058-O](https://doi.org/10.1016/0165-232X(91)90058-O))
- Paxman GJ, Tinto KJ and Austermann J (2021) Neogene-Quaternary Uplift and Landscape Evolution in Northern Greenland Recorded by Subglacial Valley Morphology. *Journal of Geophysical Research: Earth Surface*, **126**(12), e2021JF006395, ISSN 2169-9011 (doi: [10.1029/2021JF006395](https://doi.org/10.1029/2021JF006395))
- Peters LE, Anandakrishnan S, Alley RB and Smith AM (2007) Extensive storage of basal meltwater in the onset region of a major West Antarctic ice stream. *Geology*, **35**(3), 251–254, ISSN 0091-7613 (doi: [10.1130/G23222A.1](https://doi.org/10.1130/G23222A.1))
- Podolskiy EA and Walter F (2016) Cryoseismology (doi: [10.1002/2016RG000526](https://doi.org/10.1002/2016RG000526))

- Porter C, Morin P, Howat I, Noh MJ, Bates B, Peterman K, Keesey S, Schlenk M, Gardiner J, Tomko K, Willis M, Kelleher C, Cloutier M, Husby E, Foga S, Nakamura H, Platson M, Wethington Jr M, Williamson C, Bauer G, Enos J, Arnold G, Kramer W, Becker P, Doshi A, D'Souza C, Cummins P, Laurier F and Bojesen M (2018) ArcticDEM. *Polar Geospatial Center, University of Minnesota* (doi: 10.7910/DVN/OHHUKH)
- Rada C and Schoof C (2018) Channelized, distributed, and disconnected: Subglacial drainage under a valley glacier in the Yukon. *Cryosphere*, **12**(8), 2609–2636, ISSN 19940424 (doi: 10.5194/TC-12-2609-2018)
- Ranganathan M and Minchew B (2024) A modified viscous flow law for natural glacier ice: Scaling from laboratories to ice sheets. *Proceedings of the National Academy of Sciences of the United States of America*, **121**(23), e2309788121, ISSN 10916490 (doi: <https://doi.org/10.1073/pnas.2309788121>)
- Rasmussen LA and Campbell WJ (1973) Comparison of Three Contemporary Flow Laws in a Three-Dimensional, Time-Dependent Glacier Model. *Journal of Glaciology*, **12**(66), 361–373, ISSN 0022-1430 (doi: 10.3189/S0022143000031786)
- Rempel AW and Meyer CR (2019) Premelting increases the rate of regelation by an order of magnitude. *Journal of Glaciology*, **65**(251), 518–521, ISSN 0022-1430 (doi: 10.1017/JOG.2019.33)
- Renfrew IA, Elvidge AD and Edwards JM (2019) Atmospheric sensitivity to marginal-ice-zone drag: Local and global responses. *Quarterly Journal of the Royal Meteorological Society*, **145**(720), 1165–1179, ISSN 1477-870X (doi: 10.1002/QJ.3486)
- Rice JR, Lapusta N and Ranjith K (2001) Rate and state dependent friction and the stability of sliding between elastically deformable solids. *Journal of the Mechanics and Physics of Solids*, **49**(9), ISSN 00225096 (doi: 10.1016/S0022-5096(01)00042-4)
- Rippin DM (2013) Bed roughness beneath the Greenland ice sheet. *Journal of Glaciology*, **59**(216), 724–732, ISSN 0022-1430 (doi: 10.3189/2013JOG12J212)
- Ritz C, Edwards TL, Durand G, Payne AJ, Peyaud V and Hindmarsh RC (2015) Potential sea-level rise from Antarctic ice-sheet instability constrained by observations. *Nature* **2015** 528:7580, **528**(7580), 115–118, ISSN 1476-4687 (doi: 10.1038/nature16147)
- Robin Gd (1976) Is the Basal Ice of a Temperate Glacier at the Pressure Melting Point? *Journal of Glaciology*, **16**(74), 183–196, ISSN 0022-1430 (doi: 10.3189/S002214300003152X)
- Roldan-Blasco JP, Gimbert F, Gagliardini O and Gilbert A (2022) The feedback of solid friction on glacier sliding does not substantially modify the form of the friction law. *Authorea Preprints* (doi: 10.1002/ESSOAR.10507257.1)
- Rousselot M and Fischer UH (2005) Evidence for excess pore-water pressure generated in subglacial sediment: Implications for clast ploughing. *Geophysical Research Letters*, **32**(11), 1–5, ISSN 1944-8007 (doi: 10.1029/2005GL022642)
- Ruina A (1983) Slip instability and state variable friction laws. *Journal of Geophysical Research: Solid Earth*, **88**(B12), 10359–10370, ISSN 2156-2202 (doi: 10.1029/JB088IB12P10359)
- Ryser C, Lüthi MP, Andrews LC, Hoffman MJ, Catania GA, Hawley RL, Neumann TA and Kristensen SS (2014) Sustained high basal motion of the Greenland ice sheet revealed by borehole deformation. *Journal of Glaciology*, **60**(222), 647–660, ISSN 0022-1430 (doi: 10.3189/2014JOG13J196)
- Schmalholz SM and Duretz T (2015) Shear zone and nappe formation by thermal softening, related stress and temperature evolution, and application to the Alps. *Journal of Metamorphic Geology*, **33**(8), 887–908, ISSN 1525-1314 (doi: 10.1111/JMG.12137)
- Schohn CM, Iverson NR, Zoet LK, Fowler JR and Morgan-Witts N (2025) Linear-viscous flow of temperate ice. *Science*, **387**(6730), 182–185, ISSN 10959203 (doi: 10.1126/SCIENCE.ADP7708/SUPPL\_{\\_}FILE/SCIENCE.ADP7708\_{\\_}SM.PDF)
- Schoof C (2005) The effect of cavitation on glacier sliding. *Proceedings of the Royal Society A: Mathematical, Physical and Engineering Sciences*, **461**(2055), 609–627, ISSN 14712946 (doi: 10.1098/RSPA.2004.1350)
- Schoof C (2010) Ice-sheet acceleration driven by melt supply variability. *Nature*, ISSN 0028-0836 (doi: 10.1038/nature09618)
- Schoof CG and Clarke GK (2008) A model for spiral flows in basal ice and the formation of subglacial flutes based on a Reiner-Rivlin rheology for glacial ice. *Journal of Geophysical Research: Solid Earth*, **113**(B5), ISSN 2156-2202 (doi: 10.1029/2007JB004957)
- Schulson EM and Duval P (2009) Creep and fracture of ice. *Creep and Fracture of Ice*, **9780521806206**, 1–401 (doi: 10.1017/CBO9780511581397)
- Seroussi H, Nakayama Y, Larour E, Menemenlis D, Morlighem M, Rignot E and Khazendar A (2017) Continued retreat of Thwaites Glacier, West Antarctica, controlled by bed topography and ocean circulation. *Geophysical Research Letters*, **44**(12), 6191–6199, ISSN 1944-8007 (doi: 10.1002/2017GL072910)
- Seroussi H, Nowicki S, Payne AJ, Goelzer H, Lipscomb WH, Abe-Ouchi A, Agosta C, Albrecht T, Asay-Davis X, Barthel A, Calov R, Cullather R, Dumas C, Galton-Fenzi BK and others (2020) IS-MIP6 Antarctica: A multi-model ensemble of the Antarctic ice sheet evolution over the 21st century. *The Cryosphere*, **14**(9), 3033–3070, ISSN 19940424 (doi: 10.5194/TC-14-3033-2020)
- Sevestre H and Benn DI (2015) Climatic and geometric controls on the global distribution of surge-type glaciers: implications for a unifying model of surging. *Journal of Glaciology*, **61**(228), 646–662, ISSN 0022-1430 (doi: 10.3189/2015JOG14J136)
- Shreve RL (1984) Glacier Sliding at Subfreezing Temperatures. *Journal of Glaciology*, **30**(106), 341–347, ISSN 0022-1430 (doi: 10.3189/S002214300006195)

- Siegert MJ, Ross N and Le Brocq AM (2016) Recent advances in understanding Antarctic subglacial lakes and hydrology. *Philosophical Transactions of the Royal Society A: Mathematical, Physical and Engineering Sciences*, **374**(2059), ISSN 1364503X (doi: 10.1098/RSTA.2014.0306)
- Sizova E, Gerya T, Brown M and Perchuk LL (2010) Subduction styles in the Precambrian: Insight from numerical experiments. *Lithos*, **116**(3-4), 209–229, ISSN 0024-4937 (doi: 10.1016/J.LITHOS.2009.05.028)
- Slaymaker O and Kovanen DJ (2017) Pleistocene Landscapes of Western Canada. 27–48, Springer, Cham, ISBN 978-3-319-44595-3 (doi: 10.1007/978-3-319-44595-3\_{\\_}2)
- Sole A, Nienow P, Bartholomew I, Mair D, Cowton T, Tedstone A and King MA (2013) Winter motion mediates dynamic response of the Greenland Ice Sheet to warmer summers. *Geophysical Research Letters*, **40**(15), 3940–3944, ISSN 00948276 (doi: 10.1002/grl.50764)
- Souchez R, Bouzette A, Clausen HB, Johnsen SJ and Jouzel J (1998) A stacked mixing sequence at the base of the Dye 3 Core, Greenland. *Geophysical Research Letters*, **25**(11), 1943–1946, ISSN 00948276 (doi: 10.1029/98GL01411)
- Souchez R, Vandenschrick G, Lorrain R and Tison JL (2000) Basal ice formation and deformation in central Greenland: A review of existing and new ice core data. *Geological Society Special Publication*, **176**, 13–22, ISSN 03058719 (doi: 10.1144/GSL.SP.2000.176.01.02)
- Souchez R, Petit JR, Jouzel J, Simões J, De Angelis M, Barkov N, Stiévenard M and Vimeux F (2002) Highly deformed basal ice in the Vostok core, Antarctica. *Geophysical Research Letters*, **29**(7), 40–1, ISSN 1944-8007 (doi: 10.1029/2001GL014192)
- Stearns LA and Van Der Veen CJ (2018) Friction at the bed does not control fast glacier flow. *Science*, **361**(6399), 273–277, ISSN 10959203 (doi: 10.1126/science.aat2217)
- Stevens NT, Zoet LK, Hansen DD, Alley RB, Roland CJ, Schwans E and Shepherd CS (2024) Icequake insights on transient glacier slip mechanics near channelized subglacial drainage. *Earth and Planetary Science Letters*, **627**, 118513, ISSN 0012-821X (doi: 10.1016/J.EPSL.2023.118513)
- Stokes CR (2018) Geomorphology under ice streams: Moving from form to process. *Earth Surface Processes and Landforms*, **43**(1), 85–123, ISSN 1096-9837 (doi: 10.1002/ESP.4259)
- Swinzow GK (1962) Investigation of Shear Zones in the Ice Sheet Margin, Thule Area, Greenland. *Journal of Glaciology*, **4**(32), 215–229, ISSN 0022-1430 (doi: 10.3189/S0022143000027416)
- Tackley PJ (2000) Self-consistent generation of tectonic plates in time-dependent, three-dimensional mantle convection simulations 1. Pseudoplastic yielding. *Geochem. Geophys. Geosyst.*, **1**, 1021 (doi: 10.1029/2000GC000036)
- Tarasov L and Peltier WR (2007) Coevolution of continental ice cover and permafrost extent over the last glacial-interglacial cycle in North America. *Journal of Geophysical Research: Earth Surface*, **112**(F2), 2–08, ISSN 2156-2202 (doi: 10.1029/2006JF000661)
- Tedstone AJ, Nienow PW, Gourmelen N, Dehecq A, Goldberg D and Hanna E (2015) Decadal slowdown of a land-terminating sector of the Greenland Ice Sheet despite warming. *Nature*, **526**(7575), 692–695, ISSN 0028-0836 (doi: 10.1038/nature15722)
- Theakstone WH (1967) Basal Sliding and Movement Near the Margin of the Glacier Østerdalsisen, Norway. *Journal of Glaciology*, **6**(48), 805–816, ISSN 0022-1430 (doi: 10.3189/S0022143000020116)
- Thompson AC (2020) An experimental study of debris-bed friction during glacier sliding (doi: 10.31274/ETD-20200624-140)
- Thompson AC, Iverson NR and Zoet LK (2020) Controls on Subglacial Rock Friction: Experiments With Debris in Temperate Ice. *Journal of Geophysical Research: Earth Surface*, **125**(10), e2020JF005718, ISSN 2169-9011 (doi: 10.1029/2020JF005718)
- Thompson LG, Yao T, Davis ME, Henderson KA, Mosley-Thompson E, Lin PN, Beer J, Synal HA, Cole-Dai J and Bolzan JF (1997) Tropical climate instability: The last glacial cycle from a Qinghai-Tibetan ice core. *Science*, **276**(5320), 1821–1825, ISSN 00368075 (doi: https://doi.org/10.1126/science.276.5320.1821)
- Thorsteinsson T, Kipfstuhl J, Eicken H, Johnsen SJ and Fuhrer K (1995) Crystal size variations in Eemian-age ice from the GRIP ice core, Central Greenland. *Earth and Planetary Science Letters*, **131**(3-4), 381–394, ISSN 0012-821X (doi: 10.1016/0012-821X(95)00031-7)
- Tison JL, Petit JR, Barnola JM and Mahaney WC (1993) Debris entrainment at the ice-bedrock interface in sub-freezing temperature conditions (Terre Adélie, Antarctica). *Journal of Glaciology*, **39**(132), 303–315, ISSN 0022-1430 (doi: 10.3189/S0022143000015963)
- Tison JL, Souchez R, Wolff EW, Moore JC, Legrand MR and De Angelis M (1998) Is a periglacial biota responsible for enhanced dielectric response in basal ice from the Greenland Ice Core Project ice core? *Journal of Geophysical Research: Atmospheres*, **103**(D15), 18885–18894, ISSN 2156-2202 (doi: 10.1029/98JD01107)
- Trevers M, Payne AJ and Cornford SL (2024) Application of a regularised Coulomb sliding law to Jakobshavn Isbræ, West Greenland. *EGU sphere*
- Tsai VC, Stewart AL and Thompson AF (2015) Marine ice-sheet profiles and stability under Coulomb basal conditions. *Journal of Glaciology*, **61**(226), 205–215, ISSN 0022-1430 (doi: 10.3189/2015JOG14J221)

- Tsai VC, Smith LC, Gardner AS and Seroussi H (2021) A unified model for transient subglacial water pressure and basal sliding. *Journal of Glaciology*, **68**(268), 390–400, ISSN 0022-1430 (doi: 10.1017/JOG.2021.103)
- Tulaczyk S, Kamb WB and Engelhardt HF (2000) Basal mechanics of Ice Stream B, west Antarctica: 1. Till mechanics. *Journal of Geophysical Research: Solid Earth*, **105**(B1), 463–481, ISSN 2156-2202 (doi: 10.1029/1999JB900329)
- Tyndall J and Huxley TH (1857) On the structure and motion of glaciers. *Philosophical Transactions of the Royal Society of London*, **147**, 327–346, ISSN 0261-0523 (doi: 10.1098/RSTL.1857.0016)
- van den Ende MP, Chen J, Ampuero JP and Niemeijer AR (2018) A comparison between rate-and-state friction and microphysical models, based on numerical simulations of fault slip. *Tectonophysics*, **733**, 273–295, ISSN 0040-1951 (doi: 10.1016/J.TECTO.2017.11.040)
- Vaughan DG, Smith AM, Nath PC and Le Meur E (2003) Acoustic impedance and basal shear stress beneath four Antarctic ice streams. *Annals of Glaciology*, **36**, 225–232, ISSN 0260-3055 (doi: 10.3189/172756403781816437)
- Vincent C and Moreau L (2016) Sliding velocity fluctuations and subglacial hydrology over the last two decades on Argentière glacier, Mont Blanc area. *Journal of Glaciology*, **62**(235), 805–815, ISSN 0022-1430 (doi: 10.1017/JOG.2016.35)
- Vincent LA, Wang XL, Milewska EJ, Wan H, Yang F and Swail V (2012) A second generation of homogenized Canadian monthly surface air temperature for climate trend analysis. *Journal of Geophysical Research: Atmospheres*, **117**(D18), n/a–n/a, ISSN 01480227 (doi: 10.1029/2012JD017859)
- Vivian R and Bocquet G (1973) Subglacial Cavitation Phenomena Under the Glacier D'Argentière, Mont Blanc, France. *Journal of Glaciology*, **12**(66), 439–451, ISSN 0022-1430 (doi: 10.3189/S0022143000031853)
- Walder J and Hallet B (1979) Geometry of Former Subglacial Water Channels and Cavities. *Journal of Glaciology*, **23**(89), 335–346, ISSN 0022-1430 (doi: 10.3189/S0022143000029944)
- Waller RI (2001) The influence of basal processes on the dynamic behaviour of cold-based glaciers. *Quaternary International*, **86**(1), 117–128, ISSN 1040-6182 (doi: 10.1016/S1040-6182(01)00054-4)
- Walter F, Deichmann N and Funk M (2008) Basal icequakes during changing subglacial water pressures beneath Gornergletscher, Switzerland. *Journal of Glaciology*, **54**(186), 511–521, ISSN 0022-1430 (doi: 10.3189/002214308785837110)
- Walter F, Canassy PD, Husen S and Clinton JF (2013) Deep icequakes: What happens at the base of alpine glaciers? *Journal of Geophysical Research: Earth Surface*, **118**(3), ISSN 21699011 (doi: 10.1002/jgrf.20124)
- Weertman J (1957) On the sliding of glaciers. *Journal of Glaciology*, **3**(21), 33–38, ISSN 0022-1430 (doi: 10.1017/S0022143000024709)
- Weertman J (1961) Mechanism for the Formation of Inner Moraines Found Near the Edge of Cold Ice Caps and Ice sheets. *Journal of Glaciology*, **3**(30), 965–978, ISSN 0022-1430 (doi: 10.3189/S0022143000017378)
- Weertman J (1967) Sliding of nontemperate glaciers. *Journal of Geophysical Research*, **72**(2), 521–523, ISSN 2156-2202 (doi: 10.1029/JZ072I002P00521)
- Weertman J (1979) The Unsolved General Glacier Sliding Problem. *Journal of Glaciology*, **23**(89), 97–115, ISSN 0022-1430 (doi: 10.3189/S0022143000029762)
- Welty E, Zemp M, Navarro F, Huss M, Fürst JJ, Gärtner-Roer I, Landmann J, Machguth H, Naegeli K, Andreassen LM, Farinotti D and Li H (2020) Worldwide version-controlled database of glacier thickness observations. *Earth System Science Data*, **12**(4), 3039–3055, ISSN 18663516 (doi: 10.5194/ESSD-12-3039-2020)
- Whillans IM and Jezek KC (1987) Folding in the Greenland Ice Sheet. *Journal of Geophysical Research: Solid Earth*, **92**(B1), 485–493, ISSN 2156-2202 (doi: 10.1029/JB092IB01P00485)
- Wiens DA, Anandakrishnan S, Winberry JP and King MA (2008) Simultaneous teleseismic and geodetic observations of the stick-slip motion of an Antarctic ice stream. *Nature* **2008** 453:7196, **453**(7196), 770–774, ISSN 1476-4687 (doi: 10.1038/nature06990)
- Wilch E and Hughes TJ (2000) Calculating basal thermal zones beneath the Antarctic ice sheet. *Journal of Glaciology*, **46**(153), 297–310, ISSN 0022-1430 (doi: 10.3189/172756500781832927)
- Wilkens N, Behrens J, Kleiner T, Rippin D, Rückamp M and Humbert A (2015) Thermal structure and basal sliding parametrisation at Pine Island Glacier - A 3-D full-Stokes model study. *Cryosphere*, **9**(2), 675–690, ISSN 19940424 (doi: 10.5194/TC-9-675-2015)
- Willis IC (1995) Intra-annual variations in glacier motion: a review. *Progress in Physical Geography: Earth and Environment*, **19**(1), 61–106, ISSN 03091333 (doi: 10.1177/030913339501900104)
- Wilson CJ and Sim HM (2002) The localization of strain and c-axis evolution in anisotropic ice. *Journal of Glaciology*, **48**(163), 601–610, ISSN 0022-1430 (doi: 10.3189/172756502781831034)
- Winberry JP, Anandakrishnan S, Alley RB, Bindschadler RA and King MA (2009) Basal mechanics of ice streams: Insights from the stick-slip motion of Whillans Ice Stream, West Antarctica. *Journal of Geophysical Research: Earth Surface*, **114**(F1), 1016, ISSN 2156-2202 (doi: 10.1029/2008JF001035)
- Winkelmann R, Martin MA, Haseloff M, Albrecht T, Bueler E, Khroulev C and Levermann A (2011) The Potsdam Parallel Ice Sheet Model (PISM-PIK) - Part 1: Model description. *Cryosphere*, **5**(3), 715–726, ISSN 19940416 (doi: 10.5194/TC-5-715-2011)

Winter A, Steinhage D, Creyts TT, Kleiner T and Eisen O (2019) Age stratigraphy in the East Antarctic Ice Sheet inferred from radio-echo sounding horizons. *Earth System Science Data*, **11**(3), 1069–1081, ISSN 18663516 (doi: 10.5194/ESSD-11-1069-2019)

Woodard JB, Zoet LK, Iverson NR and Helanow C (2021) Variations in Hard-Bedded Topography Beneath Glaciers. *Journal of Geophysical Research: Earth Surface*, **126**(9), e2021JF006326, ISSN 2169-9011 (doi: 10.1029/2021JF006326)

Zhang Y, Sachau T, Franke S, Yang H, Li D, Weikusat I and Bons PD (2023) Ice Modeling Indicates Formation Mechanisms of Large-scale Folding in Greenland's Ice Sheet. *Authorea Preprints* (doi: 10.22541/ESSOAR.170224480.07642827/V1)

Zoet LK and Iverson NR (2020) A slip law for glaciers on deformable beds. *Science*, **368**(6486), ISSN 10959203 (doi: https://doi.org/10.1126/science.aaz1183)

Zoet LK, Carpenter B, Scuderi M, Alley RB, Anandakrishnan S, Marone C and Jackson M (2013) The effects of entrained debris on the basal sliding stability of a glacier. *Journal of Geophysical Research: Earth Surface*, **118**(2), 656–666, ISSN 2169-9011 (doi: 10.1002/JGRF.20052)

Zoet LK, Ikari MJ, Alley RB, Marone C, Anandakrishnan S, Carpenter BM and Scuderi MM (2020) Application of Constitutive Friction Laws to Glacier Seismicity. *Geophysical Research Letters*, **47**(21), e2020GL088964, ISSN 1944-8007 (doi: 10.1029/2020GL088964)

Zwally HJ, Abdalati W, Herring T, Larson K, Saba J and Stefan K (2002) Surface Melt-Induced Acceleration of Greenland Ice-Sheet Flow. *Science*, **297**, 218–222 (doi: 10.1126/science.1071795)

## 8 ACKNOWLEDGEMENTS

RL thanks Florent Gimbert and Ian Willis for an engaging viva at the Scott Polar Research Institute, Cambridge, which instigated investigation of some of the ideas explored here, Samuel Cook for comments on a draft manuscript, and Norges Forskningsråd for funding as part of the SINERGIS project (Norwegian Research Council Grant 314614, Simulating Ice Cores and Glacial Tracers in the Greenland Ice Sheet).

## A1 EXAMPLE EXPANSION OF $\mathcal{S}_{\mathcal{T}}$

$$\mathcal{S}_{\mathcal{T}}(x, y) = \begin{cases} \mathcal{S}_{R_{\alpha}}(\mathbf{u}_s) & \text{if } (x, y) \in R_{\alpha} \text{ only,} \\ \mathcal{S}_{R_{\beta}}(\mathbf{u}_s) & \text{if } (x, y) \in R_{\beta} \text{ only,} \\ \mathcal{S}_{R_{\gamma}}(\mathbf{u}_s) & \text{if } (x, y) \in R_{\gamma} \text{ only,} \\ \mathcal{S}_{R_{\alpha}}(\mathbf{u}_s) + \mathcal{S}_{R_{\beta}}(\mathbf{u}_s) & \text{if } (x, y) \in R_{\alpha} \cap R_{\beta} \text{ only,} \\ \mathcal{S}_{R_{\alpha}}(\mathbf{u}_s) + \mathcal{S}_{R_{\gamma}}(\mathbf{u}_s) & \text{if } (x, y) \in R_{\alpha} \cap R_{\gamma} \text{ only,} \\ \mathcal{S}_{R_{\beta}}(\mathbf{u}_s) + \mathcal{S}_{R_{\gamma}}(\mathbf{u}_s) & \text{if } (x, y) \in R_{\beta} \cap R_{\gamma} \text{ only,} \\ \mathcal{S}_{R_{\alpha}}(\mathbf{u}_s) + \mathcal{S}_{R_{\beta}}(\mathbf{u}_s) + \mathcal{S}_{R_{\gamma}}(\mathbf{u}_s) & \text{if } (x, y) \in R_{\alpha} \cap R_{\beta} \cap R_{\gamma}. \end{cases} \quad (22)$$

## A2 REASONING BEHIND LINE PLACEMENTS IN FIG. 2.

**Form drag, sediment** from Zoet and Iverson (2020) and Minchew and Joughin (2020b) based on the smallest clast sizes used in Zoet and Iverson (2020) but assumed to continue to sub-millimetre scales (the ice crystal size used is millimetre-scale) and extended to a reasonable but conservative upper limit for subglacial debris size. **Skin friction, sediment** from Zoet and Iverson (2020) and Minchew and Joughin (2020b) based on the size of the shear-ring apparatus used in Zoet and Iverson (2020) and extending to sub millimetre-scale of subglacial till sample used. Assumed to continue to sub-millimetre scales and to be valid at higher spatial scales given low topographic variation. **Weertman sliding** from Weertman (1957) with 1 cm to 10 m scale clearly stated in the text. **Budd** smaller-scale segment from laboratory tests in Budd and others (1979) and larger-scale segment from application to west Antarctica in Budd and others (1984). **Nye-Kamb sliding** Based on landscape used in Fig. 2 of Nye (1970). **Rate-and-state, Argentière** using assumed seismic rupture length in Helmstetter and others (2015). **Cavitation theory** from Lliboutry (1968), Gagliardini and others (2007), and Helanow and others (2021) amongst many others. Cavitation theory is often non-dimensionalised but has not exceeded the 25 m scale used in Helanow and others (2021). The dashed arrow is extended to 100 m to denote a plausible but untested upper limit to cavitation. **Intermediate scale processes** taken from the lower resolution and upper domain size used in Law and others (2023) and extended upwards with a dashed arrow to indicate an untested upper limit for the processes described. **Argentière Wheel** based on the Argentière wheel experiments of Vivian and Bocquet (1973), Gimbert and others (2021) and Gilbert and others (2023) amongst others where the glacier width is ~300 m and 20 m is roughly double the cavity length. **Skin drag** from Kyrke-Smith and others (2018) based on the lowermost resolution of radar data (40 m) to the 5 km upper limit of

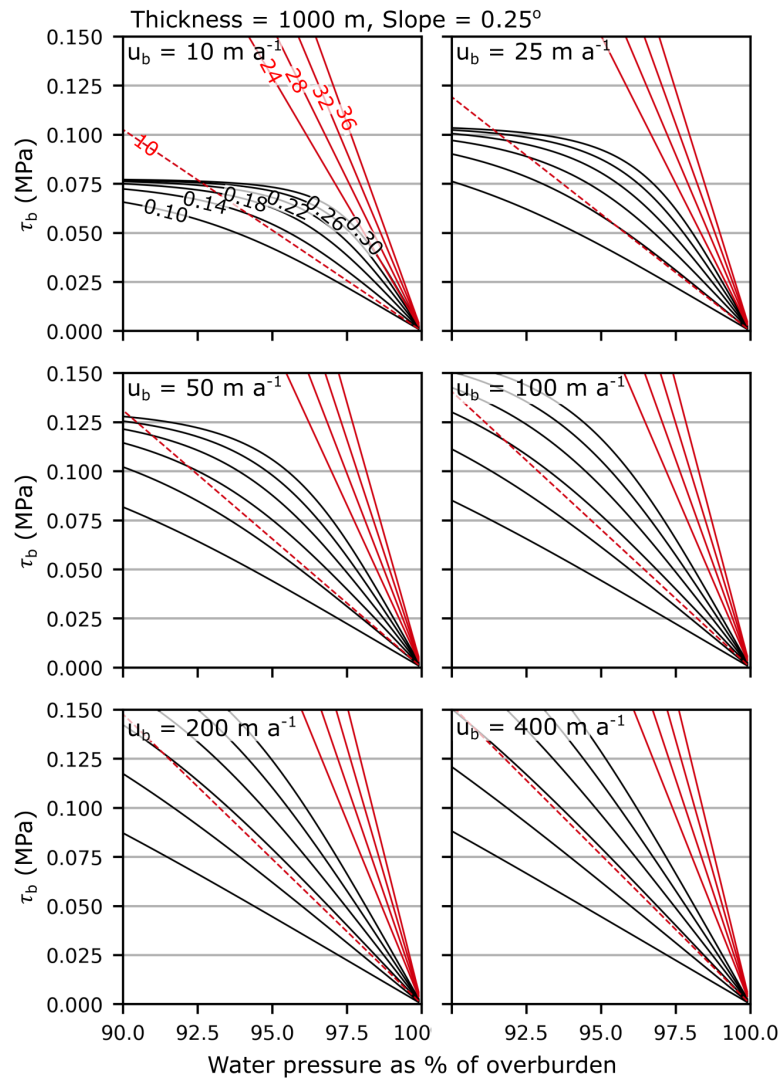


**Fig. A1.** The difference between Zoet and Iverson (2020) and Helanow and others (2021) at high water pressures.. Zoet and Iverson (2020) in red and Helanow and others (2021) in black with thickness = 1000 m and slope = 0.25° for  $u_b$  between 10 m a<sup>-1</sup> and 400 m a<sup>-1</sup>.

Bedmap2 (Fretwell and others, 2013). **Form drag, topographic** from Bingham and others (2017) and Kyrke-Smith and others (2018) using a lower radar data resolution of 40-100 m and an upper domain area of 20 km. **'Unified'**, from 1 km lower limit suggested in Tsai and others (2021) to a plausible upper limit of 10 km. **Rate-and-state, Siple Coast** Taken as broad area over which seismicity is recorded at Siple Coast in Fig. 4 of Podolskiy and Walter (2016) in contrast to single events of Helmstetter and others (2015). **Form drag, resolution/scale dependent** based on arguments within this paper (Section 3.3). **Typical glacier and ice sheet model resolution** based on standard resolutions from detailed glacier studies to coarse resolution paleo simulations. **Typical basal ice crystal size** from Thorsteinsson and others (1995) and Cook and others (2007).

### **A3 SLIDING RELATIONSHIPS IN GEODYNAMICS**

In geodynamics problems where rate-and-state friction theory is the more common way of viewing slip, models tend to use either a free-slip between mechanical layers (e.g. Sizova and others, 2010; Nakakuki and Mura, 2013), a pseudo-plastic yielding based on the coefficient of frictional sliding where boundaries between layers are not made explicit but a slip horizon is created within a continuum (e.g. Tackley, 2000; Schmalholz and Duretz, 2015), or focus on shear-localization through a non-Newtonian rheology with grain-size evolution in an initially rheologically homogeneous media (Bercovici, 2003 and references therein). These settings tend to have much more planar interfaces and do not feature the topographic variability that characterises some glacier beds, but provide interesting comparisons for glacier sliding theory.

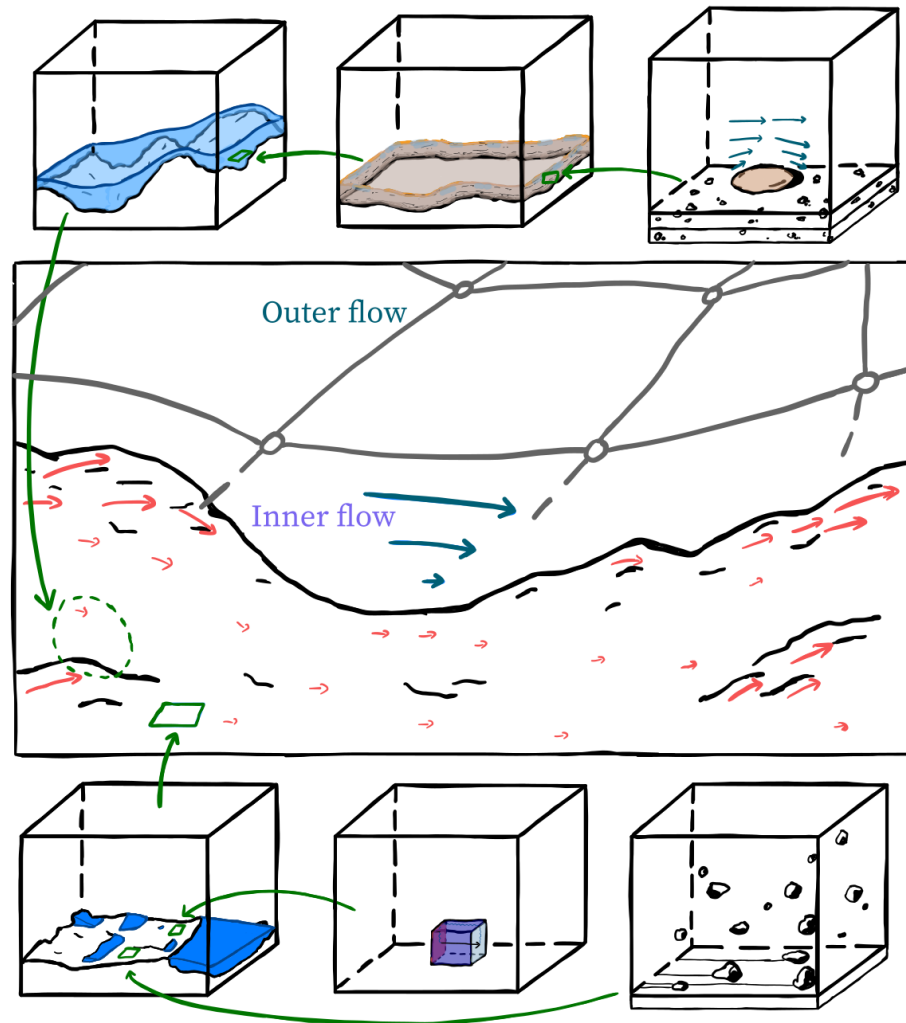


**Fig. A2.** Schematic of a set of sliding processes operating within an inner flow. Sub-processes in cubes should be recognisable from Fig. 4. Red arrows in main panel represent variable basal slip rate and blue arrows represent form drag. Grey mesh with nodes represents model grid cells at the basal boundary.

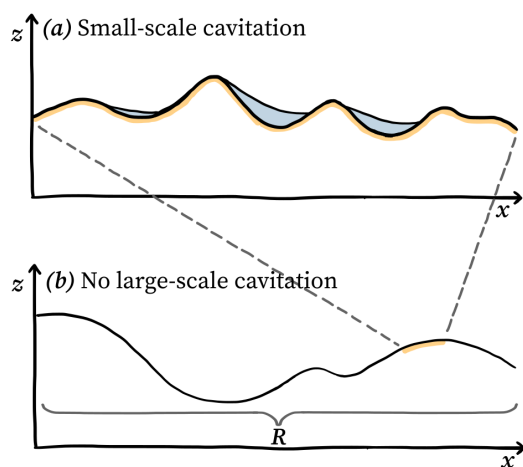


**Fig. A3.** A spatial bound to Iken's bound? **a** Cavitation (blue) occurring where topography is sufficiently small adapted from Schoof (2005). **b** Cavitation can occur at a sufficiently small scale (yellow highlight) but will not occur in larger wavelength depressions.  $z$  is height from baseline and  $x$  is distance along flow. The thick black line is the glacier bed.  $R$  represents a possible region in consideration for the sliding relationship. This figure is drawn in two dimensions for comparison with previous studies, but the same principles apply in three dimensions with realistic topography.